

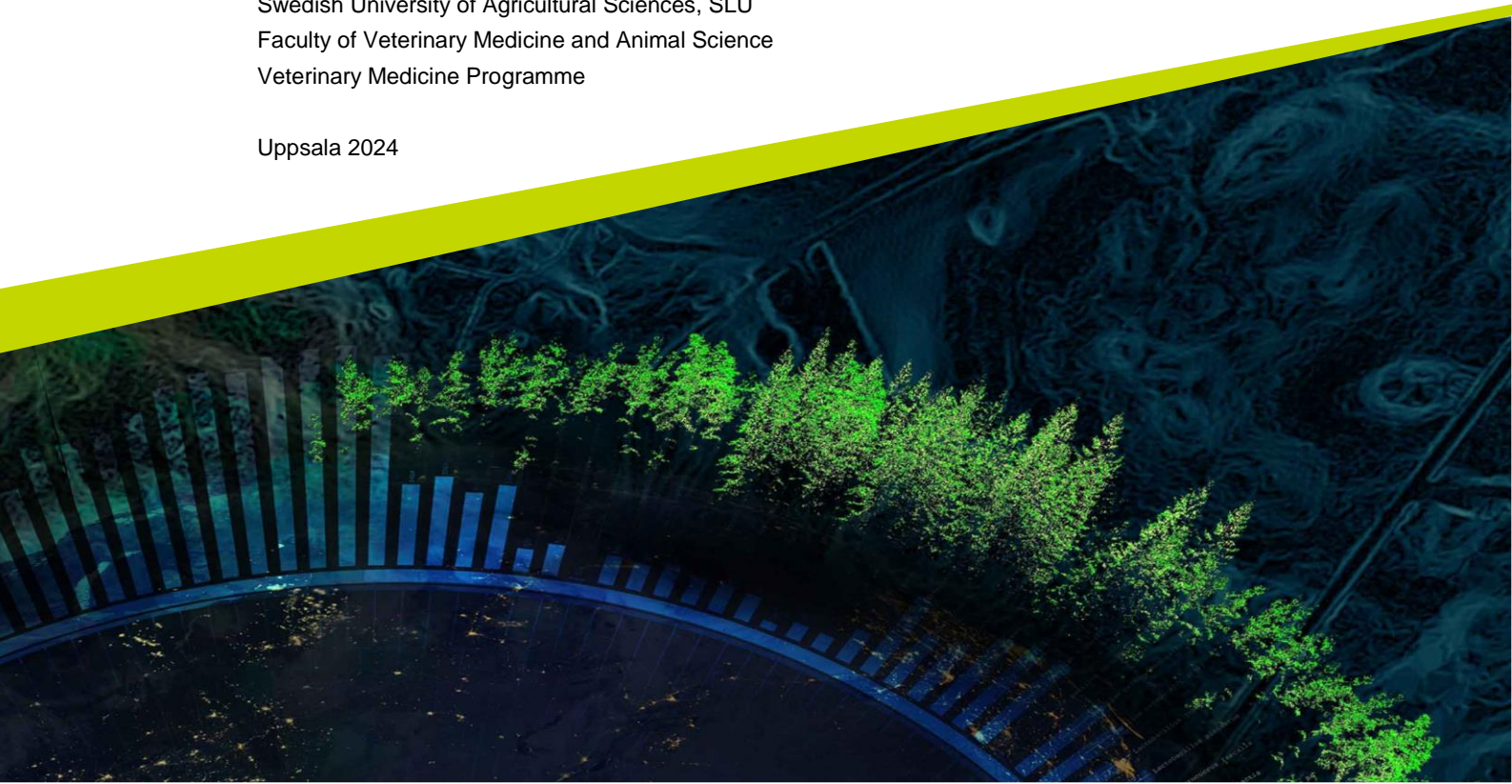


Histopathological assessment of canine lymphoma, with a focus on the inflammatory microenvironment and serglycin levels in affected lymph nodes

Evelina Sjö

Independent Project • 30 credits
Swedish University of Agricultural Sciences, SLU
Faculty of Veterinary Medicine and Animal Science
Veterinary Medicine Programme

Uppsala 2024



Histopathological assessment of canine lymphoma, with a focus on the inflammatory microenvironment and serglycin levels in affected lymph nodes

Histopatologisk bedömning av lymfom hos hund, med fokus på den inflammatoriska mikromiljön och serglycinnivån i drabbade lymfknotor

Evelina Sjö

Supervisor: Magnus Åbrink, Swedish University of Agricultural Sciences, Department of Biomedical Sciences and Veterinary Public Health

Assistant supervisor: Fredrik Södersten, Swedish University of Agricultural Sciences, Department of Biomedical Sciences and Veterinary Public Health

Examiner: Karin Vargmar, Swedish University of Agricultural Sciences, Department of Biomedical Sciences and Veterinary Public Health

Credits: 30 credits

Level: Second cycle, A2E

Course title: Independent Project in Veterinary Medicine

Course code: EX1003

Program/education: Veterinary Medicine Programme

Course coordinating dept.: Department of Clinical Sciences

Place of publication: Uppsala

Year of publication: 2024

Copyright: All featured images are our own material

Keywords: lymphoma, T-cells, B-cells, canine, microenvironment, inflammation, granulocytes, macrophages, immunohistochemistry, serglycin, qPCR, mitotic rate

Swedish University of Agricultural Sciences
Faculty of Veterinary Medicine and Animal Science
Veterinary Medicine Programme

Abstract

Research has shown that inflammation plays a significant role in the microenvironments of several cancer types, contributing to the pathogenesis and affecting prognosis. This study proposed an investigation of the microenvironment in canine lymphoma, where much of this is still unknown.

This study aimed to analyze the degree of inflammation, serglycin expression, and mitotic rate in formalin-fixed and paraffin-embedded lymphoma tissue from canine lymph nodes. The study utilized 13 unclassified lymphomas, classified as B or T as part of the study, along with eight controls, reactive lymph nodes with typical architecture.

The results could not provide evidence that there is inflammation in canine lymph nodes with lymphoma, however, it could neither rule out that there is an inflammation that primarily consists of lymphocytes and macrophages, (with low involvement of other inflammatory cells) since macrophages and lymphocytes were abundant in both cases and reactive controls. Of the lymphomas, seven were classified as B-type, three as T-type, and three could neither be classified as B, nor T. Serglycin expression in the lymphoma tissue was significantly lower than in the control tissue.

Initial insight into the levels of serglycin expression in canine lymphoma is provided by this study, and further investigation is required to understand its significance. The study's findings could help guide future research on canine lymphoma. Follow-up studies could include the classification and distribution of different subtypes of lymphocytes and macrophages, more cases, and lymphoma tissues from other organs. They could also include more advanced methods such as *single-cell RNA sequencing*, which can classify all cells in a tissue on transcriptome level.

Keywords: lymphoma, T-cells, B-cells, canine microenvironment, inflammation, granulocytes, macrophages, immunohistochemistry, serglycin, qPCR, mitotic rate.

Sammanfattning

Inflammation har visats ha en betydande roll i mikromiljön hos flera typer av cancer, det bidrar både till patogenesen och påverkar prognosen. Denna studie hade för avsikt att undersöka mikromiljön i lymfom hos hund, där mycket av detta fortfarande är outforskat.

Studiens huvudsakliga syfte var att analysera av graden av inflammation, mitoser och serglycinuttryck i formalinfixerad och paraffinbäddad lymfomvävnad från hundlymfknotor. Studien använde 13 oklassificerade lymfom, vilka klassificerades som B- eller T-cellslymfom som en del av studien, samt åtta kontroller vilka var reaktiva lymfknotor som uppvisade en normal arkitektur.

Studiens resultat har inte kunnat ge några tydliga belägg för att det är inflammation i lymfknotor med lymfom hos hund, men det har heller inte kunnat utesluta att det finns en inflammation där, som huvudsakligen består av lymfocyter och makrofager (med låg infiltration av andra inflammatoriska celler) eftersom lymfocyter och makrofager fanns i stort antal i bådelymfomen och de reaktiva kontrolllymfknotorna. Av lymfomen klassificerades åtta som B-cellslymfom, sju som T-cellslymfom och tre kunde varken klassas som B eller T. Serglycinuttrycket i lymfomvävnaden var signifikant lägre än i kontrollvävnaden.

Studien ger en första inblick i nivåerna av serglycinuttryck i lymfom hos hund, men ytterligare undersökning krävs för att förstå betydelsen av detta. Studiens resultat kan hjälpa till att vägleda framtida forskning om lymfom hos hund. Ytterligare studier behövs och skulle kunna innefatta klassificering och distribution av olika subtyper av lymfocyter och makrofager, större antal fall, och inkludering av andra vävnader än lymfknotor. Uppföljning av denna studie skulle också kunna innefatta mer avancerade metoder som *single-cell RNA sequencing*, med vilken man kan klassificera alla celler i en vävnad på transkriptomnivå.

Nyckelord: lymfom, T-celler, B-celler, hundmikromiljö, inflammation, granulocyter, makrofager, immunhistokemi, serglycin, qPCR, mitoser.

Contents

Abbreviations	9
1. Introduction	11
2. Literature review	12
2.1 Inflammation.....	12
2.2 Cancer.....	12
2.2.1 Metastasis.....	13
2.2.2 Cancer in dogs.....	13
2.3 Lymphoma	13
2.3.1 Lymphoma in dogs	14
2.3.2 Diagnostic methods for lymphoma	15
2.4 Normal architecture of a lymph node.....	15
2.5 Microenvironment in tumors.....	16
2.5.1 Inflammatory cells in canine lymphoma microenvironment.....	17
2.6 The role of inflammation and the immune system in cancers	18
2.6.1 How inflammation can lead to cancer.....	18
2.6.2 How the immune system can battle cancer.....	18
2.6.3 How the tumor can manipulate inflammation and the immune system to its advantage	19
2.7 Serglycin	20
2.7.1 Serglycin and tumor metastasis.....	21
2.7.2 Serglycin in lymphoma and other cancer forms in dogs.....	22
3. Materials and methods	23
3.1 Histopathology – assessment of lymph node tissues and infiltrating inflammatory cells	23
3.1.1 Choice of cases	23
3.1.2 Choice of controls	23
3.1.3 Preliminary assessment of existing tissue slides.....	24
3.1.4 Sectioning of FFPE lymph nodes and preparation	24
3.1.5 Staining strategies	24
3.1.6 Common histological stainings	25
3.1.7 Staining with antibodies - Immunohistochemistry.....	25
3.1.8 Grading scale for immunohistochemistry staining.....	25
3.1.9 Assessment with microscopy and numeric quantification of inflammatory cells.....	26
3.1.10 Mitoses.....	26
3.2 Molecular biology – Quantification of serglycin-coding RNA	26
3.2.1 Purification of tissues from paraffin	26
3.2.2 Purification of RNA from tissues.....	26

3.2.3	cDNA synthesis	27
3.2.4	qPCR	27
3.3	Compilation of data and statistical analysis	27
3.3.1	Counting the fold change in qPCR data	28
3.4	Statistics	28
4.	Results	29
4.1	Grading scale for immunohistochemistry staining	30
4.2	Classification of lymphoma	30
4.3	Mitoses	34
4.4	Degree of inflammation as measured by infiltration of inflammatory cells.....	36
4.4.1	Macrophage numbers.....	36
4.4.2	Mast cell numbers.....	38
4.4.3	Neutrophil numbers	38
4.4.4	Basophil numbers	38
4.4.5	Eosinophil numbers	39
4.5	Serglycin expression.....	40
4.6	Correlations.....	42
5.	Discussion	43
5.1	Inflammation in the tumor microenvironment.....	43
5.2	Serglycin levels	46
6.	Conclusions.....	48
	References	49
	Popular science summary.....	55
	Acknowledgements.....	57
	Appendix 1	59
	Appendix 2	60
	Appendix 3	61
	Appendix 4	62
	Appendix 5	64
	Appendix 6	66
	Appendix 7	68
	Appendix 8	70
	Appendix 9	72
	Appendix 10	74

Abbreviations

BVF	Department of Biomedical Sciences and Veterinary Public Health
SLU	Swedish University of Agricultural Sciences
RNA	Ribonucleic acid
DNA	Deoxyribonucleic acid
cDNA	Complimentary DNA
qPCR	Quantitative polymerase chain reaction
HE	Haematoxylin eosin
T-regs	T regulatory lymphocytes
T-cells	T lymphocytes
B-cells	B lymphocytes
RPS5	Ribosomal Protein S5
FFPE	Formalin-Fixed Paraffin-Embedded
RONs	Reactive oxygen and nitrogen species
ROS	Reactive oxygen species
NO	Nitric oxide

1. Introduction

Lymphoma is a type of blood cancer that can be very severe, where the tumor transformation has occurred in the lymphocytes (Nelson & Couto 2020b). Lymphoma often starts in lymph nodes or other lymphoid tissues but can also affect many other organs such as the liver, intestines, and skin. Being malignant it typically metastasizes, leading to survival time from a few weeks up to a couple of year after diagnosis (Keller *et al.* 2013; Valli *et al.* 2013), however, more indolent forms also exist (Flood-Knapik *et al.* 2013).

While the immune system has several ways it can take up the fight against cancer, recent research has shown that tumors can escape this by affecting the immune system and the degree of inflammation in their own micro-environmental niche (Carbone *et al.* 2014). Tumors are believed to facilitate their own growth and metastasis by influencing inflammatory functions to their advantage. The intersections of inflammation, the immune system, and cancer is a highly interesting and relevant research topic today, and immunotherapy is one of the most promising new therapies against cancer (Dagher *et al.* 2023). Therefore, this type of research has a strong connection to the clinic. By understanding the pathogenesis better, key role elements can be discovered, which, in the future, may be used as diagnostic tools or treatment methods for our dogs.

The overall aim of this case-control study is: To learn more about lymphoma in dogs, on a cellular and molecular level, and thereby increase our understanding of the inflammation's role inside the tumors. The material will be collected from the pathologist's archive of FFPE tissues. Histopathological analysis will be performed on the tissues in order to quantify the number of various inflammatory cell types and analyze the distribution of these. Additionally, the material will be analyzed with qPCR to measure the serglycin levels, and mitoses will be counted. Several specific questions are adressed in this study: Firstly, whether there is a higher infiltration of inflammatory cells in the lymphoma compared to the controls? And if so, how is this inflammation characterized? Secondly, whether there is altered serglycin expression in the lymphoma compared to the controls? And thirdly, whether there are any correlations between the infiltration of inflammatory cells, serglycin levels and mitotic rate?

2. Literature review

2.1 Inflammation

Inflammation is a complex biological response to harmful stimuli characterized by a combination of molecular and cellular events (Chen *et al.* 2017). The macroscopic symptoms of acute inflammation include the five cardinal symptoms: redness, swelling, pain, heat, and loss of function. However, at the microscopic level, inflammation is defined as an increased vascular permeability and the arrival and build-up of leukocytes, also called inflammatory cells, which release inflammatory mediators such as cytokines.

2.2 Cancer

Cancer is a disease that occurs when cells undergo genetic changes that cause them to divide uncontrollably (Newkirk *et al.* 2017). In some way, cancer cells escape the strict regulations that all other cells in the body are under. Another characteristic of cancer cells is that they are not properly differentiated, meaning they lose their specific function and appearance. Although any cell type in the body can become neoplastic, frequently dividing cell types are at increased risk. Every time a mitosis occurs, the sensitive DNA is unraveled, a risk moment where mutations can occur if something goes wrong. Several mutations are needed for a cell to become neoplastic. Often, neoplastic cells lead to the formation of a mass, a so-called tumor or neoplasia. A tumor that only grows in the site where it originated is called benign, but if it invades surrounding tissues and can spread to other places in the body, it is called malignant. Malignant forms often spreads to other distant places and forms new tumors, which are called metastases. A benign tumor can become a malignant one, and as time goes by, not only does the maternal tumor get more extensive, but the risk of the tumor spreading also increases, therefore, early detection of the disease is essential to improve chances of survival.

2.2.1 Metastasis

Metastasis is a complex multi-step process requiring several mutations to be successful (Breen & Cullen 2020). While some cells may acquire the ability to break away from the primary tumor, this does not automatically mean that they can migrate through the extracellular matrix. Nor does it necessarily mean they can attach to the basement membrane of a vessel, secrete proteases to damage its vessel barrier, penetrate it, and enter the blood or lymph stream. Once they have intravasated, the tumor cells must survive in the circulation and avoid being detected and eliminated by the immune system. Eventually, they must also be able to exit the vessel and establish themselves in a new location. Despite extensive research, the exact mechanisms of how tumor cells behave in these steps, and under what circumstances, remain to be discovered.

2.2.2 Cancer in dogs

Cancer is a common cause of death for many dogs, with up to 60% mortality rate in some breeds (Nelson & Couto 2020a). The Golden Retriever is a breed that belongs to the most affected ones. However, many dogs can be treated and sometimes even cured using surgical removal. And now, with advances in veterinary medicine, medical therapies will likely become more available over time, giving new hope (Bergman 2019).

2.3 Lymphoma

Lymphoma is a type of blood cancer that originates from tumor-transformed lymphocytes (Vail *et al.* 2019), these cells are a crucial part of the adaptive immune system commonly found in lymph nodes or the circulation. The first symptom of lymphoma is often enlarged lymph nodes. Lymph nodes can, however, also be enlarged for other reasons. Further symptoms may include weight loss, fever, lethargy, inappetence, polyuria/polydipsia, vomiting, swelling or breathing difficulties, depending on which organs are affected (Zandvliet 2016). There are two main types of lymphoma, B-cell lymphoma, and T-cell lymphoma, depending on which type of lymphocyte has been tumor-transformed (Boes & Durham 2017). However, there is also a type known as non-B non-T lymphoma where the cell types can no longer be classified. There are numerous specific subtypes that lymphoma can be further divided into based on histopathological criteria. However, it is important to mention that there is not always a global consensus about these. The World Health Organization (WHO) has a classification system for canine lymphomas that can be utilized. A proper diagnosis is essential as symptoms, prognosis, and treatment may vary. The next part will focus on a few individual subtypes of lymphoma, which are the most common in dogs.

2.3.1 Lymphoma in dogs

Out of all cancers diagnosed in dogs, 7-24% are estimated to be some type of lymphoma (Vail *et al.* 2019). Lymphoma can appear in four manifestations: multicentric, mediastinal, alimentary, or cutaneous. Multicentric lymphoma, where several lymph nodes are involved and sometimes also other organs, is a common manifestation in dogs and accounts for over 80%.

Diffuse large B-cell lymphoma is, by far, the most common form of lymphoma in dogs, making up approximately 50% (Seelig *et al.* 2016; Meuten *et al.* 2020). The second most common form is peripheral T-cell lymphoma, with 15%, and then T-zone lymphoma, with 8%. Dogs of all ages can be affected, but as with many cancer forms, most patients are middle-aged or older (Nelson & Couto 2020b). The prognosis for lymphoma in dogs is generally very poor. However, it is important to remember that there are numerous different forms, including more indolent ones such as T-zone lymphoma. Indolent lymphomas have a relatively good prognosis (Flood-Knapik *et al.* 2013; Frantz *et al.* 2013), and according to Boes & Durham (2017) 29% of canine lymphomas are indolent. In a study by Valli *et al.* (2013), low-grade T-cell lymphoma had the longest median survival of 662 days, while high-grade peripheral T-cell lymphoma had the shortest median survival time of 162 days. On the contrary, another study has shown that fewer go into remission with T-cell phenotype and that those who do relapse faster (Chun *et al.* 2000). Furthermore, in a study on miniature dachshunds, which is a predisposed breed, it was seen that individuals with T-cell phenotype or older age had significantly shorter survival time compared to dogs under four years of age with B-cell lymphoma (Rimpo *et al.* 2022). Of course, the survival time also depends on how early the disease is detected, and if or how it is treated.

While cats are known to develop lymphoma due to viral infection, no similar connection has been found in dogs (Nelson & Couto 2020b). The etiology of lymphoma in dogs is thought to be multifactorial, with genetic predisposition. Heritage is suspected since certain breeds and bloodlines are significantly more affected than others and that certain types of lymphomas are more common in certain breeds. For instance, B-cell lymphoma is more common in Cocker Spaniels and Bassets, while T-cell lymphoma is more common in Boxers, Shih Tzus, and Siberian Huskies. In Golden Retriever, however, the two types are equally common. Another factor that can increase the risk of lymphoma in dogs is diseases that cause chronic inflammation, such as IBD which affects the intestines (Carbone *et al.* 2014).

2.3.2 Diagnostic methods for lymphoma

When diagnosing lymphoma, two methods can be used: cytology of fine needle aspirates or histopathological analysis of tissues from biopsies or whole extirpated lymph nodes, the latter with whole extirpated lymph nodes being the *gold standard* (Newkirk *et al.* 2017). Standard Hematoxylin and Eosin (HE) staining is often used to examine the sample. However, HE can only confirm a few things, namely that it is a lymphoma, as well as the degree of mitosis, and whether it consists of mostly large- or small-cells. The size refers primarily to the size of the cell nucleus, and erythrocytes are used as a size reference (Seelig *et al.* 2016). The small nuclei are rounded and dark, while the large ones are light with a few dark spots, reflecting the chromatin structure. In some instances, however, it is desired to have more detailed information about the sample, for example, what main type of lymphoma it is. To classify a lymphoma as B- or T-, immunohistochemistry is often used, a method where antibodies attach to certain cell structures and stain them, making it possible to separate cells that otherwise look the same (Cho 2022). Knowing the cell type will help the veterinarian to estimate prognosis and choose an appropriate treatment plan together with the dog owners.

2.4 Normal architecture of a lymph node

A *lymph node* is a complex organ that contains a thin fibrous capsule of fibroblasts and collagen (Pawlina 2011). Underneath the capsule lies a space known as the subcapsular sinus that receives incoming lymph fluid. Multiple afferent lymphatic vessels enter at various points through the capsule. However, there is only one efferent lymphatic vessel, and it exits via the hilus, where the vein leaves and artery enters. The capsule and subcapsular sinus sometimes descend into trabeculae, dips found between groups of follicles in the cortex. The sinuses extend down to the medulla, where they form medullary sinuses.

The outer cortex, located beneath the subcapsular sinus, contains lymph follicles with lighter germinal centers consisting mainly of B-cells and dendritic cells (Pawlina 2011). This is surrounded by a darker ring of T-cells that have less cytoplasm. Below the outer cortex lies the deep cortex, which contains mainly T-cells and high endothelial venules. In the medulla, there are medullary chords, darker islands consisting of reticular cells, plasma cells, macrophages, some B-cells, and dendritic cells. The medullary sinuses are lighter winding areas found between the medullary chords. These sinuses are spaces where lymph fluid is filtered between cells. The cells slow the flow and allow for easier capture of antigenic material. However, this mechanism can also lead to a large burden of metastatic tumor cells that can establish in the lymph node. The majority of cells in

a lymph node are lymphocytes (Pawlina 2011). Some have more cytoplasm and others less, resulting in lighter and darker areas in the lymph node. When a lymph node is reactive it is responding to lymph flow from an infected area in the body, inflammatory cells such as neutrophils, eosinophils and macrophages may then be found in the sinus with the drained lymph, but the lymph node itself is not infected by the agent (Thomas 2008; Valli *et al.* 2016). If the lymph node gets infected it will be inflamed, this is referred to as lymphadenitis, with inflammatory cells arriving via the blood that can be found all the way up in the cortex. Outside the capsule, lymph nodes are often encompassed by adipocytes and some smaller blood vessels (Pawlina 2011).

2.5 Microenvironment in tumors

It is crucial to understand that a tumor is not just made up of tumor cells but also various other elements (Newkirk *et al.* 2017). These elements collectively form what is known as the stroma, which includes extracellular matrix, fibroblasts, blood vessels, lymph vessels, inflammatory cells, immune cells, and molecules. When talking about the *tumor microenvironment*, it is referring to both the tumor cells and the stroma surrounding them, which can both play a significant role in the development of the tumor. Tumors are known to interact with their surroundings, and these interactions can be categorized into three types: the tumor stroma interaction, the tumor immune interaction, and paraneoplastic effects.

Tumor stroma interactions

Tumor cells can interact with the stroma and stimulate the construction of new blood vessels, a process known as angiogenesis (Newkirk *et al.* 2017). Inducing angiogenesis is crucial for tumor growth, as a solid tumor cannot expand beyond two millimeters without neovascularization (Carmeliet & Jain 2000). Regarding the *tumor stroma interactions* specifically, there seem to be three major pattern types applying to tumor cells in lymphoma microenvironments, as described by Burger *et al.* (2009): An independent type, where the cells no longer need external signals to divide. A dependent type, where the cells rely on certain flaws in their surroundings (such as control mechanisms flaws) to divide. A third type is where the cells are instead driven by external stimuli, such as cytokines or cell interactions in the surroundings, which trigger the proliferation.

Tumor immune interactions

Tumor immune interactions involve a delicate balance between the immune system and tumor cells (Newkirk *et al.* 2017). While the immune system strives to recognize and eliminate the tumor cells, the tumor cells use diverse strategies to

sidestep or suppress the immune system, sometimes even by direct cell-to-cell interactions, for example, in blockage of lymphocyte receptors.

Paraneoplastic effects

Tumors not only inflict mechanical pressure on the surrounding tissues and deplete the functional parenchyma of the organs they grow in, but they can also excrete molecules/factors, causing paraneoplastic effects (Newkirk *et al.* 2017). These effects can impact the entire body, even if they are derived from just a single solid tumor, leading to for example anemia, cachexia, or hypercalcemia.

2.5.1 Inflammatory cells in canine lymphoma microenvironment

T-regulatory lymphocytes (T-regs) and their role in B lymphoma was investigated in a study by Pinheiro *et al.* (2014). The results showed that T-regs were significantly increased in the tumors in the livers and spleens, leading to reduced anti-tumor responses and a worse prognosis for the patient. The study suggested that T-regs could play a crucial role in the pathogenesis of the disease. However, it was also highlighted that the tumor microenvironment may vary across different types of lymphoma.

Mast cells in canine lymph node lymphoma was studied in a research by Woldemeskel *et al.* (2014). They showed that mast cells were significantly increased and associated with higher tumor microvessel density in lymphoma lymph node tissue.

Macrophages were studied in a recent study on lymph node lymphoma by Vázquez *et al.* (2021), which revealed that high-grade lymphomas had higher portions of M2 macrophages, most evident in T-cell lymphomas. However, the highest number of both M1 and M2 macrophages was observed in B-cell lymphomas. It was also observed that the population of macrophages varied depending on the degree of the lymphoma.

Eosinophils were examined by Ozaki *et al.* (2006) which found that eosinophils were present in all cases of intestine T-cell lymphoma that were included in the study.

Neutrophils in the microenvironment of canine lymphoma, have, to the best of our knowledge, not yet been studied thoroughly. However, a recent study that investigated the relationship between neutrophilia in blood and the prognosis of canine lymphoma patients suggested that this aspect should be explored further in

future studies (Veluvolu *et al.* 2021). Although there were indications, the study did not find a significant correlation between neutrophilia and worse prognosis.

2.6 The role of inflammation and the immune system in cancers

2.6.1 How inflammation can lead to cancer

During inflammation, reactive oxygen and nitrogen species (RONS) are produced by immune cells and used as a weapon against infectious agents (Kay *et al.* 2019). However, these RONS can also unintentionally harm neighboring cells and tissues. Due to their strong reactivity, RONS can damage DNA, increasing the risk of mutations and exacerbating inflammation. Moreover, apart from the RONS secreted, intracellular RONS can also arise from pro-inflammatory cytokine cascades.

Fortunately, a cellular system is already in place to repair DNA damage (Kay *et al.* 2019). This system is extremely important. Even under normal conditions, approximately ten point mutations occur in every mitosis. This number is even higher in cases of inflammation due to the reactions described above. In addition, (immune)-cells divide more frequently during inflammation to replace the cells lost in the battle, providing more opportunities per time unit for something to go wrong. Usually, these repair system run smoothly and work excellently. However, if they get disrupted so that the DNA damages are not mended, mutations gathering up could lead to cancer. There are some particular components of this repair process that inflammation has been known to disrupt. For instance, RONS can react with proteins in the repairing enzymes, preventing them from functioning properly.

In some cases, genome damage can trigger necroptosis, a programmed cell death that leads to an inflammatory response (Kay *et al.* 2019). This response is caused by the exposure of inner cell fragments, parts that are typically always concealed inside the cell. These are recognized as damage-associated molecular patterns (DAMPs) that activates for example, macrophages, mast cells, neutrophils, and lymphocytes.

2.6.2 How the immune system can battle cancer

The immune system can recognize cancer cells and kill them through various mechanisms, sometimes even leading to tumor destruction in the early stages (Munhoz & Postow 2016). Interestingly, our immune systems have probably defeated cancer cells numerous times without us even knowing it.

Some immune cells have been identified as particularly effective in fighting cancer cells, such as natural killer cells, cytotoxic T-cells, B-cells, and M1 macrophages (Munhoz & Postow 2016). Nevertheless, first they have to recognize the presence of a tumor cell. T-cells, for example, need to interact with an antigen presented on MHC to be activated. Neoantigens are abnormal proteins that never exist in the body normally but appear due to disturbances inside the tumor cell. If neoantigens are presented on MHC molecules, this can alert T-cells and initiate an attack. In some cases, tumor cells can downregulate their expression of MHC, thereby escaping the threat of T-cells (Wolf *et al.* 2023). In these instances, cancer cells may instead be killed by Natural Killer (NK) cells, specialized in killing any cells that do not express normal MHC.

The cytotoxic M1 macrophages can recognize and kill a cancer cell by releasing nitric oxide (NO) and reactive oxygen species (ROS), generally taking 1-3 days per cell (Pan *et al.* 2020). They can also identify a cancer cell by antibodies that are attached to it, via a mechanism called antibody dependent cellular cytotoxicity (ADCC), and this helps the macrophages to eliminate it in a much faster process, taking just a few hours. The antibodies against tumor cells are produced by B-cells. Additionally, macrophages recruit more NK cells and boost them to kill.

2.6.3 How the tumor can manipulate inflammation and the immune system to its advantage

Two immune cells seem to play a crucial role in protection of tumors: T-regs and M2 macrophages (Kim *et al.* 2020). While these two cell types are normally an essential part of balanced immune responses, tumors appear to recruit them to the tumor site and promote their differentiation. T-regs can facilitate tumor growth by downregulating inflammation and the immune-mediated anti-tumor response, mainly by secretion of cytokines such as TGF- β and IL-10. High T-reg numbers in the tumor microenvironment are directly associated with shorter survival times in numerous cancer types. M2 macrophages can enhance tumor growth by releasing cytokines such as growth factors (e.g. epithelial growth factor and fibroblast growth factors), which bind to cell surfaces and transduce a signal to stimulate proliferation (Pan *et al.* 2020). Besides, M2 macrophages secrete molecules that degrade the extracellular matrix and blood vessels in tumors, thus increasing the risk of cancer cells spreading. Moreover, they can inhibit the activity of NK cells and cytotoxic T-cells.

The formation of new blood vessels is not solely an effect of the increased number of expanding cells in need of oxygen, but is also linked to pro-angiogenic factors, molecules such as VEGF-A (Carbone *et al.* 2014). These factors are synthesized and released by cancer cells in an uncontrolled manner, thereby stimulating angio-

genesis in the tumor microenvironment. The new vessels facilitate further growth of the tumor. Hence, the growing tumor drives the neovascularization in a positive feedback loop. However, this process is further stimulated by other factors, such as M2 macrophages, that are known to be pro-angiogenic, but also by other pro-inflammatory conditions created by various immune cells. The new vessels are often abnormal and have increased permeability due to leakages, which probably facilitates the extravasation of tumor cells and metastasizing (Breen & Cullen 2020). The leakage also results in tissue edema and increased intra-tumoral pressure, as well as slow blood flow in the vessels and decreased perfusion, leading to hypoxia and necrosis, which causes inflammation.

Immune checkpoint inhibitors are something that cancer cells may use to turn off cytotoxic T-cells (Buchbinder & Desai 2016). It is a way in which the antitumor response is downregulated: The tumor cells express PD-L1, a molecule that, when it binds to the PD-1 receptor on T-cells, induces programmed cell death in the T-cell. Another down regulatory pathway is by the CTLA-4 receptor which binds to the B7 (CD80/CD86), which transduces an inhibitory signal in the T-cell that makes it less active. The PD-1 and CTLA-4 receptors are important features on the T-cells to keep homeostasis and balanced immune responses. However, tumor cells expressing PD-L1 and B7 molecules that bind to these receptors will trick the system and have a severe advantage.

T-cell exhaustion is a phenomenon that can occur in various situations, including chronic inflammation and tumor microenvironments, often in long periods of high antigen load (Wherry 2011). Although it is still not fully understood, it seems that a reduction of helper T-cells (CD4+) can exacerbate cytotoxic T-cell exhaustion, leading to attenuation in the T-cells' ability to kill cancer cells and to secrete cytokines such as IL-1.

2.7 Serglycin

Serglycin is a type of proteoglycan, meaning it is a protein with long unbranched negatively charged sugar chains attached to it (Kolset & Tveit 2008). It is predominantly located intracellularly and is particularly abundant in inflammatory cells. One of its primary functions is to aid in forming secretory vesicles and granules. However, it is believed that serglycin also may serve several other purposes.

2.7.1 Serglycin and tumor metastasis

A study conducted in 1995 discovered that serglycin, which is secreted in granular form from hematopoietic cells, acts as a ligand for CD44 and that these two molecules interact to enable lymphocytes to adhere and get activated (Toyama-Sorimachi *et al.* 1995). It was also observed that different cell types express different isoforms of CD44 and serglycin, and this variation could result in different effects between different cell types. When serglycin binds to CD44, it rearranges the cytoskeleton, leading to focal adhesion turnover, which promotes migration and may facilitate metastasis in tumor cells (Guo *et al.* 2020). Targeting of serglycin could therefore, be a possible approach in future therapies.

Serglycin also plays a crucial role in the cargo loading of tumor cell exosomes, as highlighted by Purushothaman *et al.* (2017). Knock-out of the serglycin gene in tumor cells resulted in exosomes that could not provide an invasive phenotype or trigger macrophage invasion. This discovery also suggests that targeting serglycin could be a possible way to reduce cancer progression and metastasis.

In murine models of breast cancer, a striking finding was made by Roy *et al.* (2016). They found that genetic knock-out of serglycin in mice with mammary cancer resulted in these individuals getting no metastases to the lungs at all, in difference to the control mice that did get metastases. Furthermore, the knock-out did not have any effect on the growth of the primary tumors in the udders, leading to the conclusion that serglycin must be crucial for metastasis in this cancer form, at least in mice.

In nasopharyngeal carcinoma cancer, high levels of serglycin have been observed to correlate with increased motility and metastatic potential (Li *et al.* 2011). In cells overexpressing serglycin, this potential and the motility increased even more. With siRNA mediated knock-out, it was decreased. Similarly, in hepatocellular carcinoma, serglycin seems to have an important role in the pathogenesis, where a higher level of serglycin was linked to worse clinical outcomes (He *et al.* 2013). Furthermore, in osteosarcoma, a study by Lv *et al.* (2021) found that cells with upregulated serglycin had significantly increased proliferation and invasion, which was reduced after knock-out. They also suggested a connection between serglycin and the Jak/STAT signaling pathway.

On the contrary, as it might seem, higher histological grades of breast cancer in humans were significantly linked to lower serglycin levels, with the interpretation that low serglycin levels, in an independent manner, could predict poor prognosis (Hosoya *et al.* 2022).

In immune cells, serglycin plays an important role in the maturation of the dense-core cytotoxic granules in cytotoxic T-cells and NK-cells, as well as transporting and storing of perforin and granzyme B, two cytotoxic effector molecules (Sutton *et al.* 2016). In these cell types, cytotoxicity was severely limited when serglycin was poor, leading to lower levels of granzyme B in NK cells. In cytotoxic T-cells, Granzyme B and perforin were both lowered. Serglycin is, in other words, essential for the function of immune cells that target cancer cells.

2.7.2 Serglycin in lymphoma and other cancer forms in dogs

To our knowledge, serglycin has not previously been studied in canine lymphoma. However, various studies have examined serglycin expression in other types of neoplasia in dogs. An increase in serglycin compared to healthy control tissue was seen in mastocytoma, spleen hemangiosarcoma and malignant mammary neoplasia (Jönsson 2019; Djerf 2022; Linder 2022). Interestingly, in benign mammary neoplasia, the serglycin levels were low, even lower than the controls (Jönsson 2019).

3. Materials and methods

3.1 Histopathology – assessment of lymph node tissues and infiltrating inflammatory cells

3.1.1 Choice of cases

In this case-control study, cases of spread lymphoma in dogs were located by searching the journal database and documented lists of the pathologists archived biobank at BVF. Lymphoma tissues from different organs such as lymph nodes, skin, intestines, spleens, and livers were considered, and the stained slides were picked up from storage for a preliminary view of the samples. In the end, lymph nodes were considered the most suitable as they were affected in most patients and were relatively homogenous, which would simplify the counting of cells since we aimed to count ten fields in 40 x magnification on the objective and 10 x magnification on the ocular (2.37 mm²). Furthermore, sections should ideally look relatively the same even after 20 cuts in the paraffin blocks. The liver would have been our second choice since it was also affected in a majority of the lymphoma patients. However, the localization in the livers was mainly periportal in areas too small to even cover a full field of 40 x magnification, which would have complicated the cell counting.

An initial idea was to use normal/tumor free tissue in the periphery of each section as individual-specific controls, but this proved impossible. In all the organs with lymphoma, tumor cells were more or less diffusely spread in the whole sample, even when the main localization was focal.

3.1.2 Choice of controls

For the controls, the same database was searched, primarily looking for dogs that had been autopsied with any diagnosis and where a lymph node had been saved. Those with any type of neoplasia in the autopsy report were sorted out, as well as those with any kind of immune-related diagnosis. We initially called these lymph

nodes normal lymph nodes, but they all proved to be more or less reactive, which led us to call them reactive control lymph nodes instead.

3.1.3 Preliminary assessment of existing tissue slides

A list was conducted with all the dogs' lymph node lymphomas. Together with a senior pathologist, the pre-existing HE sections were reviewed in detail. Those that were moderate to severely autolytic were sorted out since we suspected they might give unreliable stainings in immunohistochemistry and misleading results in the qPCR method. Only the mildly autolytic samples were retained, yielding 13 lymphomas and eight controls. There was no prospect of doing a random case selection since we already had so few cases. However, ideally, we would have included many more randomly chosen cases. In this study, time was a limiting factor in how many cases could be located and processed. All the cases and controls had an autopsy code and were randomly given a blinded working number between 1-21. The material from necropsies and biopsies used in this study dated from 2017 to 2023.

3.1.4 Sectioning of FFPE lymph nodes and preparation

The paraffin blocks containing the relevant formalin fixed material were gathered from the archive. In some cases, multiple organs were included in the same block, and in those cases, the blocks were melted so the lymph nodes could be collected and placed individually in blocks. From each of these 21 lymph nodes, approximately 20 sections, each 4 μm thick, were sectioned and mounted on glass slides. Two sections were placed on each slide, and the slices were then stored in boxes for easy retrieval whenever staining was performed.

3.1.5 Staining strategies

For each lymph node, the first and last slices were stained with HE to examine that the tissue morphology still looked fairly the same. Next, we utilized the rest of the slices to stain with acidic Toluidine blue (mast cells), Giemsa (mast cells), IBA-1 (macrophages), CD3 (T-cells) and CD20 (B-cells) to investigate the presence and distribution of various cell types. Apart from the eight reactive control tissues, we also included a positive control lymph node in each run to ensure that the immunohistochemistry method was working, avoiding false negatives. We used the lower section on each slice as a negative control to confirm that the staining observed in the upper section was due to the actual primary antibody (antigen specific) and not any other factor. Furthermore, we also took measures to avoid false positives by checking for the presence of other brown pigments, such as melanin, before we started.

3.1.6 Common histological stainings

Standard protocols for HE-, Giemsa- and Toluidine stainings with some lab-specific adjustments were used in this study, see Appendix 1-3. HE staining is particularly useful in highlighting tissue architecture and identifying various types of cells, such as eosinophils, neutrophils, basophils, and lymphocytes. In healthy tissue, identifying these cells is relatively straightforward. However, in tumor tissue, this might be more challenging since the cells are not always fully or correctly differentiated. Despite this, mitoses can still be counted with relative ease.

3.1.7 Staining with antibodies - Immunohistochemistry

In some cases, normal histological staining methods may not be sufficient to distinguish between different cell types. Immunohistochemistry can then be used when a particular cell type is of interest. It is a method based on primary antibodies and a detection system, such as ENVISION. In this study primary antibodies were utilized that were monoclonals produced in mouse or rabbit hybridoma, working against human CD-markers. These antibodies were chosen based on their ability to cross-react with the canine orthologs, confirmed through Biocompare Antibody search and feedback comments on the producer's product page. Before the start of the project, tests were also conducted on dog tissues using these antibodies, which yielded excellent results. All antibodies used in this study and the ENVISION detection system were purchased from DAKO. See Appendix 4-6 for detailed information on the batch number, concentrations, and protocols.

3.1.8 Grading scale for immunohistochemistry staining

Rather than grading the staining as mild, moderate or severe, the number of stained cells was graded on a scale from 0 to 5. The scale was designed as part of the study and is shown in Table 1. Figure 1 under *Results* will show some examples of gradings according to the scale.

Table 1. Definition of the immunohistochemistry staining scale.

Staining scale	Percentage of stained cells
0 =	< 1%
1 =	1 - 19%
2 =	20 - 39%
3 =	40 - 59%
4 =	60 - 79%
5 =	80 -100%

3.1.9 Assessment with microscopy and numeric quantification of inflammatory cells

Histopathological assessment of the 21 cases and controls were conducted together with a senior pathologist, and cells were counted in ten fields of 40 x enlargement on the objective and 10 x magnification on the ocular (2.37 mm²) on all samples. All the counting was performed in the same microscope for comparability. Pictures were taken of several representative sections as illustrations of the results.

3.1.10 Mitoses

To accurately count mitoses, ten fields of 40 x magnification on the objective and 10 x magnification on the ocular (2.37 mm²) were used. The counting process began in the lower left corner and continued moving up from side to side, ensuring that the same area was not counted twice. As per the guidelines of diagnostic pathology practice, the counting was focused where the mitotic activity appeared to be the highest. The counting process was performed blinded to avoid bias. Codes on the slices did not reveal whether it was a case or a control. An article by Donovan et al. (2021) that provided numerous pictures was used as a guideline when identifying mitotic figures. In addition, educational materials from Veterinary Cancer Guidelines and Protocols (2022) were used to practice correctly separating mitotic figures from mitotic-like figures. A senior pathologist also supported the counting process.

3.2 Molecular biology – Quantification of serglycin-coding RNA

3.2.1 Purification of tissues from paraffin

For this part of the study, the blocks used previously were utilized to cut 20 µm thick sections, two or more from each sample, depending on how much tissue was left in the block. The smaller the lymph node tissue, the more sections were taken as compensation to get approximately the same total tissue area. The tissues in these sections were then purified from paraffin using the protocol described in Appendix 7.

3.2.2 Purification of RNA from tissues

If there was a production of serglycin within the cells, this could be revealed by the remaining RNA-strands in the cytoplasm, coding for serglycin. If there was a high production, there should be high levels of this RNA, and if there was a low production, there should be low levels of this RNA. In this step, RNA was purified from the tissue using the Trizol/chloroform method with an added step of Nucleo-

spin RNA clean-up XS. The latter was used to receive a higher RNA quality. The full protocol can be seen in Appendix 8. Amongst the RNA purified in this step, there is of course, apart from the possible RNA coding for serglycin, a myriad of other RNA coding for other proteins as well.

3.2.3 cDNA synthesis

In this step, the RNA was transformed into cDNA using the enzyme Superscript IV (Invitrogen). This step was necessary since only DNA can be used in the qPCR machine and not RNA. Before we started synthesizing the cDNA, we made sure to have the same amount of RNA from each sample and the same volumes by first measuring the levels and then diluting every sample individually. The protocol for cDNA synthesis can be seen in appendix 9.

3.2.4 qPCR

qPCR (quantitative polymerase chain reaction) is a method used to show the presence and quantity of a particular DNA sequence. It works by exponentially increasing the number of copies up to several millions; this means that even samples with extremely low amounts can be used. Apart from the samples, specific gene primers, nucleotides, and the thermophilic DNA-polymerase enzyme, were used in the reaction. Serglycin (SRGN) was our target gene since that was the gene we wanted to measure. Furthermore, we also included a housekeeping gene (RPS5) in a separate run with the samples. Housekeeping genes are essential for cell existence and are usually at similar levels between cells. This was used as a control for the method and as a reference for the target gene values. The samples were pipetted into a 96-well for the qPCR, with every sample in duplicate wells. This aimed to get mean values, which are more reliable than single values. It was also used as a self-control for the pipetting; if the two differed a lot, something had probably gone wrong. Several-year-old formalin-fixed material, like ours, had been used in this method before, with good results, even though it was expected to have slightly lower quality than fresh tissue or live cells. See the protocol for the qPCR in Appendix 10.

3.3 Compilation of data and statistical analysis

The data collected from each case was compiled in an Excel file. The cases were then tagged as cases and controls to identify possible differences. Data analysis was conducted using the statistical programme Prism 10 (GraphPad), which also creates graphs. These graphs and data will be presented in the next chapter.

3.3.1 Counting the fold change in qPCR data

Since there were differences in total gene expression in each tissue, this had to be taken into consideration, and this was why the values from the lymphomas could not be directly compared to the values of the controls. Therefore, we performed a Double delta CT analysis. By using the reference gene values, a ratio called *fold change* was obtained: All the values for RPS5 were added and divided by 21, giving the mean value of 32.33764. This mean value was used to compare every individual value from the serglycin batch. We took each serglycin value minus the RPS5 mean value and received delta cq values. These delta cq values were then divided with the mean value of all serglycin delta cq values, giving a delta-delta cq value for each serglycin sample. These values were then put in the formula 2^{-X} , giving us $2^{\Delta\Delta ct}$ values for each sample, which were used to illustrate the results in a diagram.

3.4 Statistics

Due to differences in various parameters, such as the degree of autolytic changes and the age of the paraffin blocks the non-parametric Mann-Whitney statistical method and Welsh t-test were considered. However, in the end, after observing that the values did follow a standard deviation, decision was taken to go with the parametric unpaired student T-test, which was used in all the diagrams shown in the *Results* chapter and gave all the p-values stated.

4. Results

The 21 patients included in this study are presented in Table 2.

Table 2. The signalments of the cases and controls that were included in this study. Ly = Lymph node, Sp* = Spleen, Lu* = Lungs, Ki* = Kidneys, St* = stomach, In* = intestines. ** Toller = Nova Scotia Duck Tolling Retriever.*

Work code	Case/control	Breed	Gender	Age (Years)	Metastases (Organs)
16	Case	Toller**	Bitch	14	Ly* Sp* Lu*
3	Case	German Sherpherd	Male	9	Ly* Sp* Lu* Ki*
20	Case	Mixed breed	Bitch	6	Ly* Sp* Li*
11	Case	Swedish Elkhound	Bitch	3	Ly* Li*
10	Case	Chinese Crested Hairles	Male	8	Ly* Li*
13	Case	Mixed breed	Male	0,8	Ly* Li*
21	Case	Shipperke	Bitch	12	Ly* Li*
2	Case	Rhodesian Ridgeback	Bitch	3	Ly* Sp* Li*
7	Case	Labrador Retriever	Bitch	7	Ly* Sp* Li* Lu* In*
1	Case	Berner Sennen	Bitch	3	Ly* Li* Ki* Lu*
8	Case	Flat Coated Retriever	Male	5	Ly* Li* St* In*
14	Case	English Bullodog	Male	7	Ly*
19	Case	Toller**	Bitch	8	Ly*
4	Control	Chihuahua	Bitch	14	-
12	Control	Labrador Retriever	Male	9	-
17	Control	Shetland Sheepdog	Male	6	-
6	Control	Staffordshire bullterrier	Male	3	-
9	Control	Berner Sennen	Bitch	5	-
18	Control	Mixed breed	Bitch	1	-
15	Control	Cocker Spaniel	Male	2	-
5	Control	Lagotto Romagnolo	Male	11	-

4.1 Grading scale for immunohistochemistry staining

The immunohistochemistry with antibodies against CD3, CD20, and IBA-1 all resulted in brown staining. Even though strong positive stainings could often be seen as a brown coloration even without the microscope examination under the microscope is crucial to see the stained cells clearly. In the microscope it is possible to see where the stain has attached, to avoid false positives, and where the stained cells are located in the section. The antibodies used in this study attached to the cytoplasm and cell membrane, but not to the nuclei. Figure 1 shows some examples of how stainings were graded according to a staining scale that was constructed in *Material and methods*. There are examples from each step on the scale except 0, which would have been a blank, or a nearly blank section.

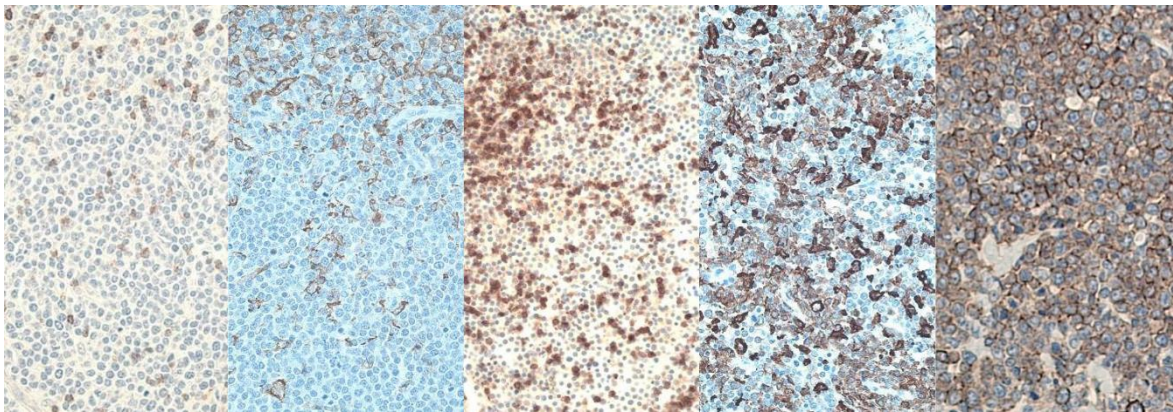


Figure 1. Images show examples of classification according to the stain scale (grade 1-5), Grade 1 = 1 - 19% stained, grade 2 = 20 - 39% stained, grade 3 = 40 - 59% stained, grade 4 = 60 - 79% stained, grade 5 = 80 - 100% stained.

4.2 Classification of lymphoma

The classification as B- or T-lymphoma was done together with an experienced senior pathologist. Without immunohistochemistry this classification would not have been possible, immunohistochemistry was performed so that both B-cells and T-cells could be identified and assessed for each lymphoma (and control). If one cell type was more abundant than the other, for example B-cells, and the B-cells had a neoplastic morphology, the majority of the mitoses, and also expanded into areas where they should not normally be located, those 4 criteria would have been enough to classify it as a B-lymphoma, in this study. To support this process and get some kind of data on the amount of stained B and T cells, the staining scale was constructed and used on all cases and controls. The results of how large amounts of

B cells and T cell were found in the lymphomas and reactive controls are shown in figure 4.

Most sections of the lymphomas had both CD3- and CD20-positive cells, even if one type was more dominant than the other. Table 3 shows how all the individual cases and controls in the study were graded and what type of lymphoma the lymphomas were classified as. Note: the percentage of stained cells was based on all the cells in the lymph node, not just the lymphocytes, there might be other cell types, also the classification was performed blinded, hence the B- cells plus the T-cells do not necessarily add up to 100%.

Amongst the 13 lymphomas, seven were classified as B, and three were classified as T. Three could be classified as neither B nor T due to poor staining with both antibodies. Some pictures with examples of how stained B cells and T cells could look in the lymph nodes can be seen in Figure 2 and 3.

Table 3. This table illustrates how all the cases and controls were graded in the CD3 and CD20 stainings, and the type (B/T) the lymphomas were classified into as part of this study. m = multifocal.*

Patient code	Case/control	CD3 scale	Distribution	CD20 scale	Distribution	Type
16	Case	1	Focal	5	Diffuse	B
3	Case	0	None	5	Diffuse	B
20	Case	1	Focal	2	Diffuse + Edge	B
11	Case	2	Generalized m*	0	None	?
10	Case	5	Diffuse	2	Generalized m*	T
13	Case	2	Generalized m*	0	None	B
21	Case	2	Focal	3	Generalized m*	B
2	Case	3	Generalized m*	0	None	T
7	Case	2	Focal	3	Generalized m*	B
1	Case	1	Focal	1	Focal	?
8	Case	0	None	2	Generalized m*	?
14	Case	0	None	4	Diffuse	B
19	Case	2	Generalized m*	1	Focal	T
4	Control	3	Cortical	1	Follicles + Edge	-
12	Control	1	Focal cortical	?	?	-
17	Control	2	Focal cortical	4	Diffuse	-
6	Control	2	Cortical	1	Focal + Edge	-
9	Control	2	Focal cortical	2	Generalized m* + Edge	-
18	Control	2	Cortical	1	Focal	-
15	Control	3	Cortical + diffuse	2	Focal	-
5	Control	1	Focal	3	?	-

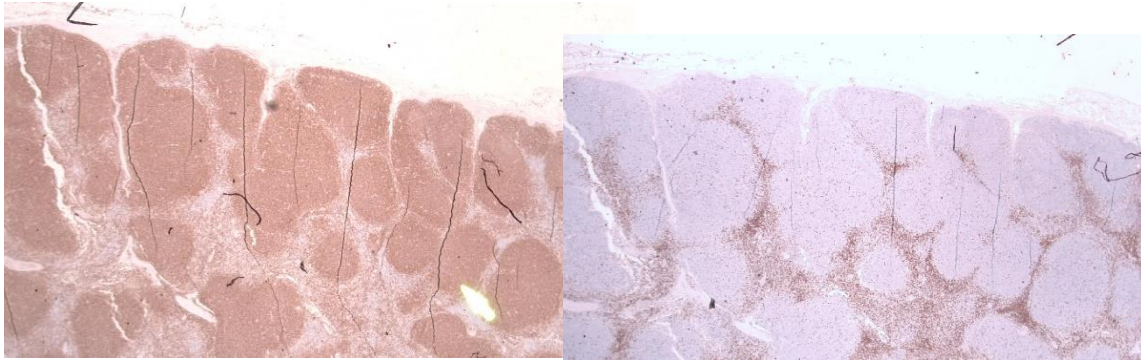


Figure 2. Here is an example of how B cells (left picture) and T cells (right picture) stained in a lymph node. On the staining scale the B cells got 3 and the T cells 2 (observe that the whole lymph node does not show on this picture) This was a lymphoma, and it was classified as a B lymphoma.

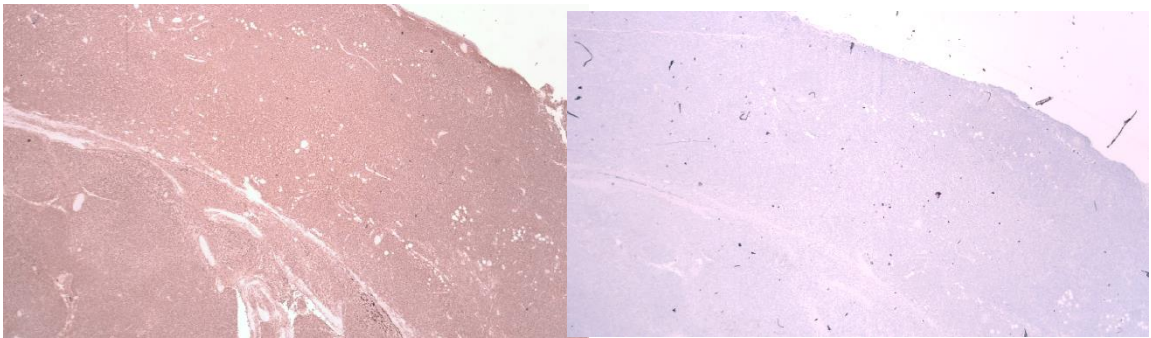


Figure 3. Here is another example of how B cell (left picture) and T cells (right picture) stained in a lymph node. On the staining scale the B cells got 5 and T cells 0 (observe that the whole lymph node does not show on this picture) This was a lymphoma, and it was also classified as a B lymphoma.

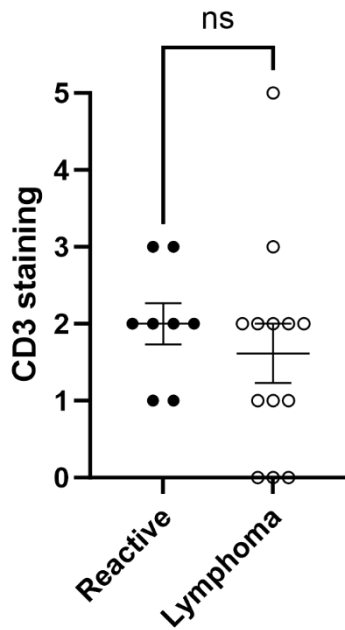


Figure 4a. Shows a non-significant difference in the staining of T-cells with CD3 between the controls and lymphomas ($P = 0.3080$ with parametric unpaired student T-test). In the reactive controls, T cells were always below 60% (3 on the scale), and often below 40% (2 on the scale). The same was true for the lymphomas, except from one case that consisted almost only of T cells, and this one was classified as a clear T-cell lymphoma.

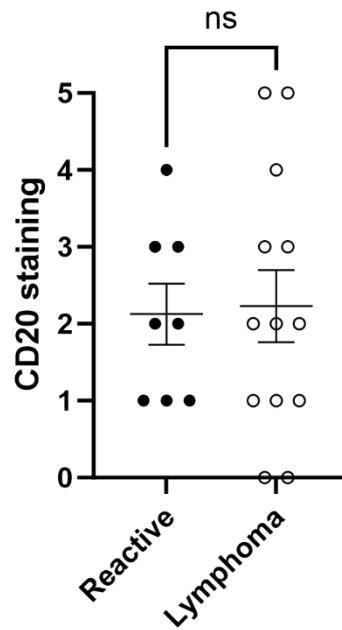


Figure 4b. Shows staining for B-cells, neither here is there a significant difference between controls and lymphomas ($P = 0.3080$ parametric unpaired student T-test). Three lymphomas had more than 60% (3 on the scale) B-cells, and these were classified as clear B-lymphomas.

4.3 Mitoses

The mitotic rate in 10 fields of 40 x magnification on the objective and 10 x magnification on the ocular (2.37 mm²) ranged between 10 and 40 mitoses in the lymphomas, with a mean value of 24. The reactive control lymph nodes ranged between 2 and 25 mitoses, with a mean value of 11. The number of mitoses for each case and control is shown in Table 4 and illustrated in Figure 6. Pictures with examples of mitotic figures that were counted can be seen in Figure 5.

Table 4. The number of mitoses for each case and control.

Patient code	Case/control	Mitoses
16	Case	29
3	Case	25
20	Case	40
11	Case	35
10	Case	32
13	Case	27
21	Case	16
2	Case	23
7	Case	22
1	Case	32
8	Case	10
14	Case	12
19	Case	10
4	Control	10
12	Control	11
17	Control	11
6	Control	2
9	Control	3
18	Control	25
15	Control	12
5	Control	12

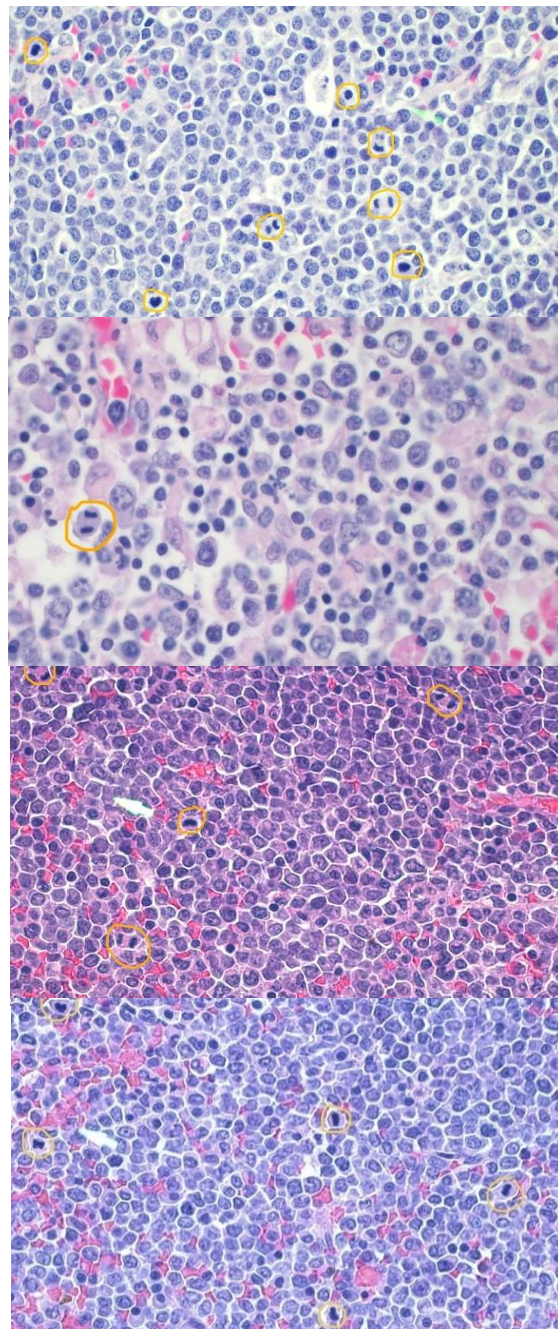


Figure 5.a-d. The images show examples of mitotic figures that were counted, observe that these were taken in the overhead microscope on 60 x enlargement and edited, while the actual counting was done on 40 x enlargement on the objective and 10 x magnification on the ocular (2.37 mm²) in a regular microscope.

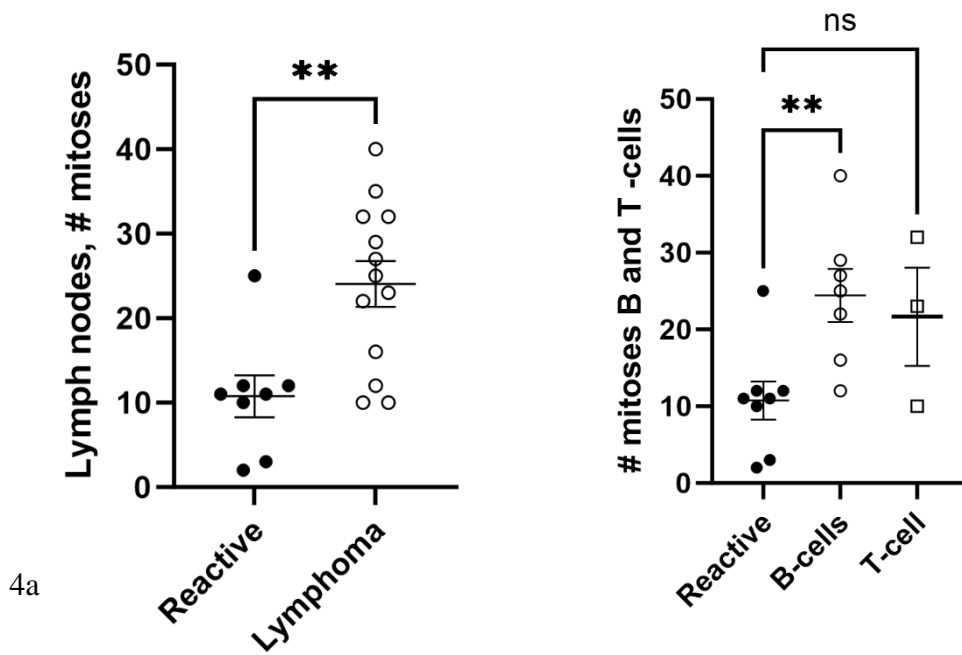


Figure 6a. Number of mitoses illustrated between reactive controls and lymphoma (P -value = 0.0034). Figure 6b. Number of mitoses illustrated between reactive controls and lymphoma divided into B- or T-lymphoma ($P = 0.0197$ with parametric unpaired student T -test).

4.4 Degree of inflammation as measured by infiltration of inflammatory cells

4.4.1 Macrophage numbers

Macrophage numbers were high in both lymphoma and reactive control lymph nodes. They stained strongly with IBA-1. The macrophages were generally abundant in the lymph nodes, except for in the follicles, where they were much fewer in both the controls and the lymphomas (the few lymphomas that still had follicle-like structures) see Figure 7-9. The macrophage distribution in the controls aligned fairly well with the expected distribution in a normal lymph node, as described by the literature. The grading of macrophages according to the grading scale is shown below in Table 5. The number of macrophages was not significantly different in the lymphomas compared to the controls as illustrated in Figure 10.

Table 5. The cases and controls and their stainings with IBA-1 according to our staining scale.

Patient code	Case/control	IBA-1	Distribution
16	Case	2	Generalized multifocal, fewer in follicles
3	Case	2	Generalized multifocal
20	Case	5	Diffuse
11	Case	3	Generalized multifocal
10	Case	2	Generalized multifocal + Edge
13	Case	2	Generalized multifocal
21	Case	2	Generalized multifocal, fewer in follicles
2	Case	2	Generalized multifocal
7	Case	3	Generalized multifocal
1	Case	3	Generalized multifocal
8	Case	3	Generalized multifocal
14	Case	2	Generalized multifocal
19	Case	2	Generalized multifocal, fewer in follicles
4	Control	3	Generalized multifocal , fewer in follicles
12	Control	2	Generalized multifocal
17	Control	3	Generalized multifocal, fewer in follicles
6	Control	3	Generalized multifocal , fewer in follicles
9	Control	2	Generalized multifocal
18	Control	3	Generalized multifocal, fewer in follicles
15	Control	3	Generalized multifocal, fewer in follicles
5	Control	3	Generalized multifocal, fewer in follicles

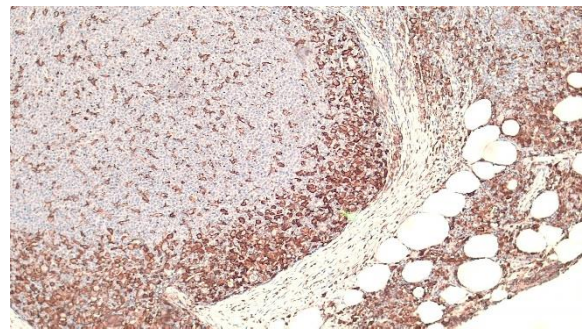
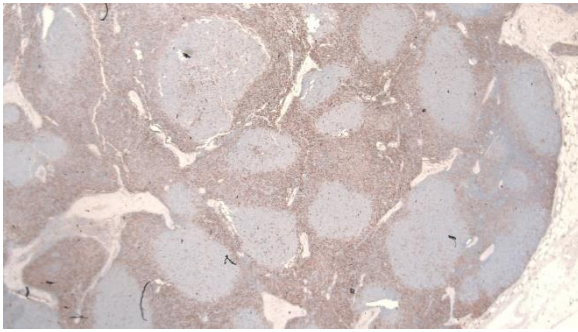


Figure 7.a. IBA-1 staining, macrophages in a lymphoma. Figure 7.b. Close up on a follicle.

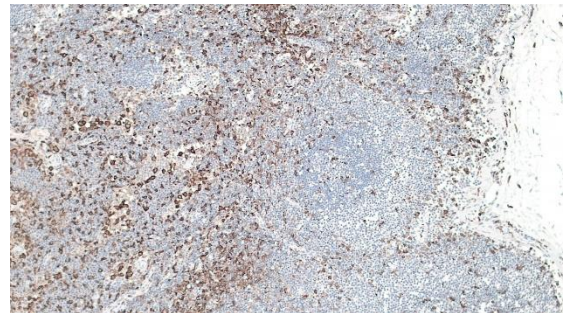
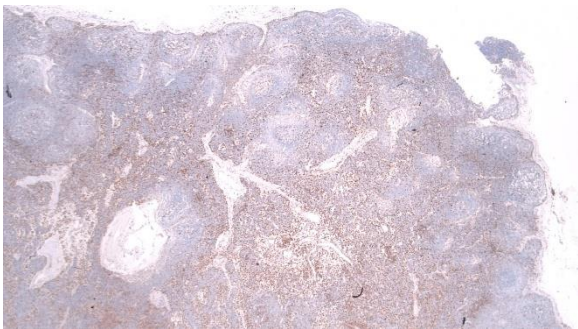


Figure 8.a. IBA-1 staining, macrophages in a reactive control. Figure 8.b. Close up on a follicle.

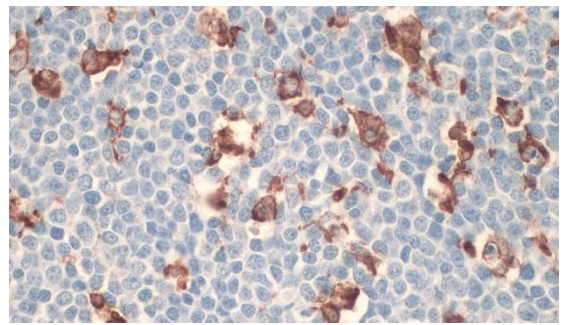
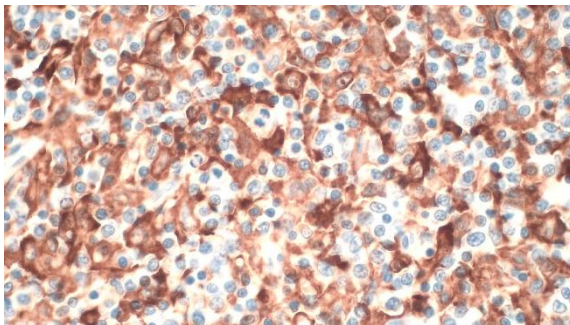


Figure 9.a. Macrophages in a macrophage dense area in a lymphoma. Figure 9.b. Macrophages in the middle of a follicle in a lymphoma.

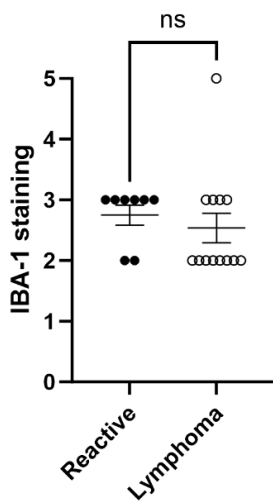


Figure 10. The diagram shows that the amount of stained macrophages were very similar between the reactive controls and the lymphomas ($P = 0.3080$ with parametric unpaired student T-test)

4.4.2 Mast cell numbers

Mast cell numbers were low in both lymphoma and reactive control lymph nodes, as shown in Table 6 and illustrated in Figure 14. However, a few were often present in the peripheral fat surrounding the lymph nodes outside the capsule and sometimes inside the lymph node in the connective tissue close to a vessel, as shown in figure 11 and 12. The mast cells outside the capsule were not counted.

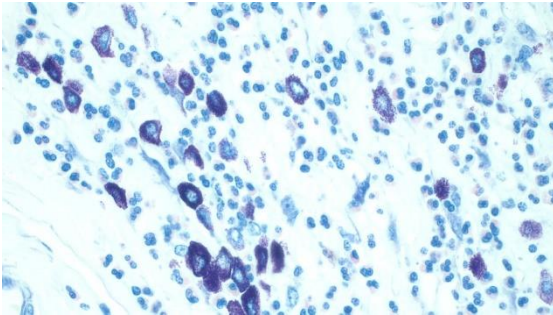


Figure 11.a. Mast cells in a positive control, showing how mast cells should ideally stain, zoomed in on high magnification to show the granula in strong purple.

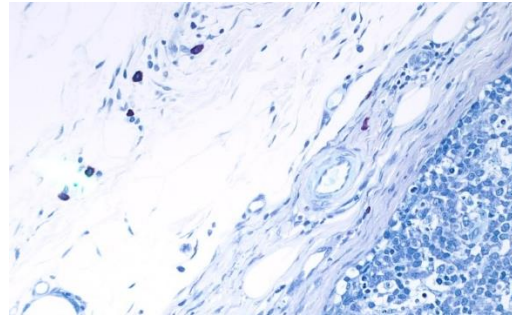


Figure 11.b. shows mast cells in the peripheral fat outside the capsule of a lymphoma, where mast cells could often be seen.

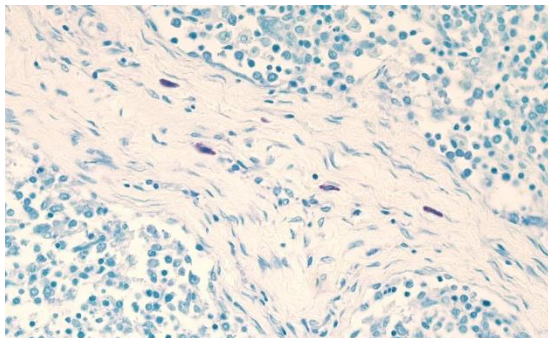


Figure 12.a. Four mast cells in the connective tissue of a lymphoma, it was rare to see this many mast cells close together in the parenchyma.

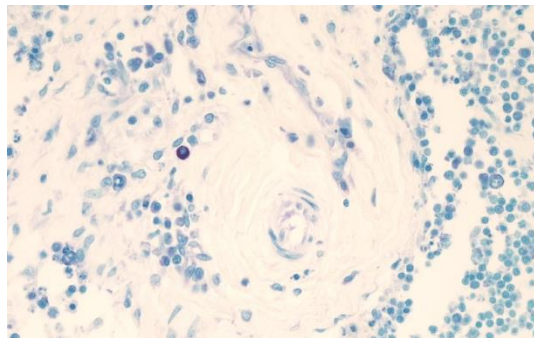


Figure 12.b. A single mast cell sits close to the connective tissue of vessel in a lymphoma, this is how the mast cells were most often encountered inside the lymph nodes.

4.4.3 Neutrophil numbers

Neutrophil numbers were very low. Rarely a couple or even a single one could be seen in the entire parenchyma. See Table 6 and Figure 14.

4.4.4 Basophil numbers

No basophils were encountered in any of the samples.

4.4.5 Eosinophil numbers

A few eosinophils were encountered in some controls and lymphomas, with red granular and segmented nuclei, see Figure 13, Table 6 and Figure 14.

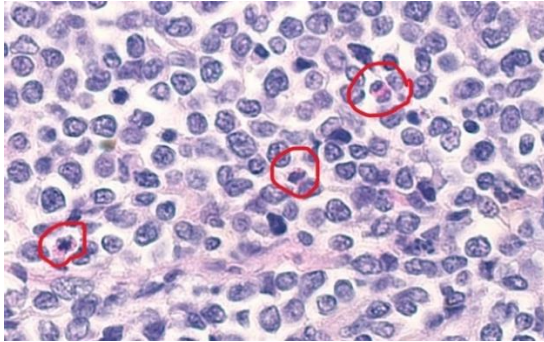


Figure 13.a. Three eosinophils in the parenchyma of a lymphoma.

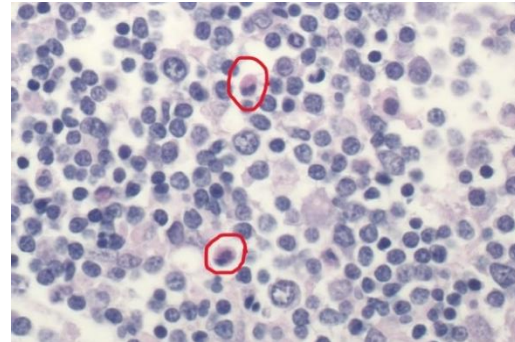


Figure 13.b. Two eosinophils in the parenchyma of a reactive control lymph node.

Table 6. Number of granulocytes present in lymph nodes.

Patient code	Case/control	Mast cells (cells)	Eosinophils (cells)	Basophils (cells)	Neutrophils (cells)
16	Case	0	1	0	0
3	Case	1	0	0	0
20	Case	0	0	0	0
11	Case	8	0	0	0
10	Case	0	5	0	0
13	Case	2	0	0	0
21	Case	6	0	0	0
2	Case	0	0	0	0
7	Case	0	0	0	0
1	Case	0	0	0	0
8	Case	0	0	0	0
14	Case	0	0	0	0
19	Case	5	0	0	0
4	Control	0	0	0	0
12	Control	0	0	0	0
17	Control	12	2	0	0
6	Control	1	0	0	2
9	Control	2	1	0	1
18	Control	14	5	0	2
15	Control	0	0	0	0
5	Control	0	0	0	0

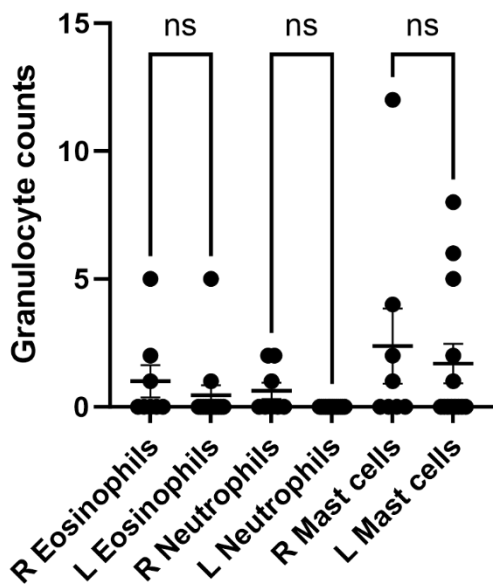


Figure 14. Number of granulocytes (inflammatory cells) in reactive control lymph nodes and lymphomas. R = reactive, L = lymphoma. Basophils were also counted but are not shown in the figure since they were 0 in both groups. There were no significant differences between the controls and lymphomas regarding these cell types ($P = 0.1517$ with parametric unpaired student T-test).

4.5 Serglycin expression

The serglycin gene (SRGN) expression was measured through a reference gene called RPS5, also known as a *house keeping gene*. Initially, the qPCR machine recorded data for each sample in the 96-well plate, and the data represented the *heating cycle* (out of a maximum of 39 cycles) at which the serglycin products were large enough to be measured. Since we had data from two wells for each sample (two wells for RPS5 and two for Serglycin), we used the mean value for each. These values can be seen in Table 7 and are illustrated in Figure 15. The statistical method used is a parametric unpaired student T-test, which gave a significant difference in the results with a p-value of 0.0088.

Table 7. Serglycin expression in the reactive controls and lymphomas.

Patient code	Case/control	RNA coding for serglycin	Housekeeping gene
16	Case	-	33.14
3	Case	35.115	28.38
20	Case	37.235	30.795
11	Case	37.29	-
10	Case	36.4	30.175
13	Case	33.405	27.44
21	Case	36.58	30.5225
2	Case	34.475	28.415
7	Case	35.945	-
1	Case	-	-
8	Case	-	-
14	Case	37.56	30.605
19	Case	37.72	35.46
4	Control	36.8	34.3
12	Control	33.6325	29.205
17	Control	34.35	29.82
6	Control	34.95667	32.7075
9	Control	36.08667	34.14667
18	Control	-	-
15	Control	37.56	-
5	Control	-	33.84667

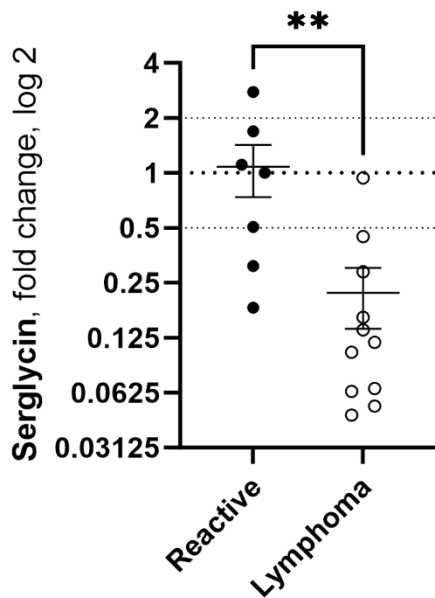


Figure 15. Serglycin expression in the reactive controls and lymphomas. (P-value = 0.0088 with parametric unpaired student T-test)

4.6 Correlations

Correlations were tested between serglycin levels and the number of mitoses since these were the only two factors with significant differences, the factors of age and gender were also added as a bonus. Each patient is represented by a coloured circle, see Figure 16. The only tendency to a correlation was between higher mitotic rate and lower serglycin levels.

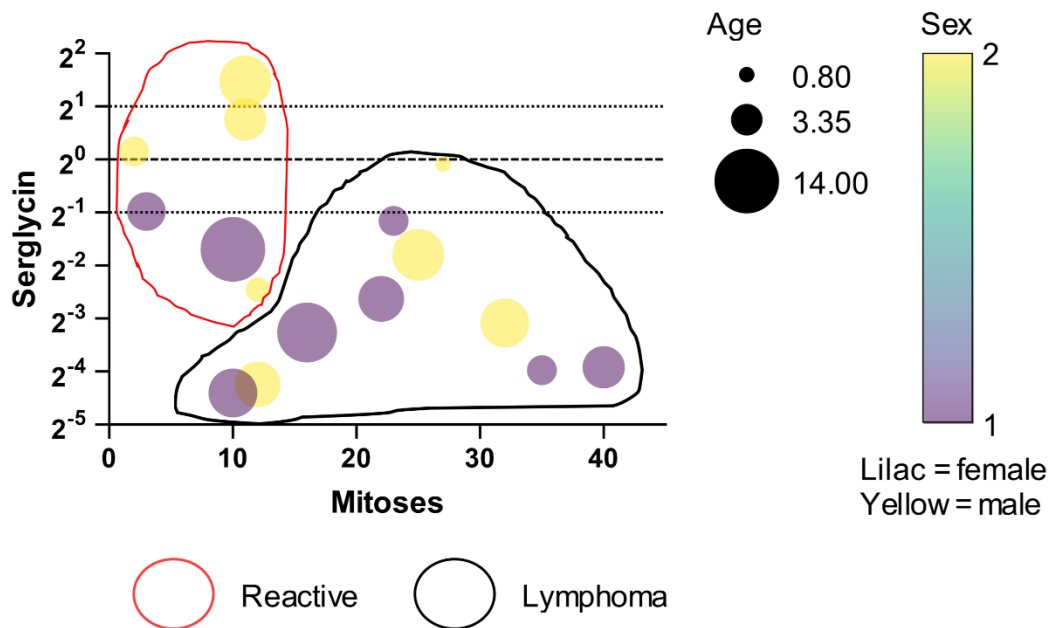


Figure 16. Correlations between serglycin levels and number of mitoses in the cases and controls. Age and sex are added as additional factors highlighted by the size and colors of the rings.

5. Discussion

5.1 Inflammation in the tumor microenvironment

Regarding lymphoma in dogs specifically, there are a few studies that have assessed individual inflammatory cell types in the microenvironment (Ozaki *et al.* 2006; Pinheiro *et al.* 2014; Woldemeskel *et al.* 2014; Vázquez *et al.* 2021), but none that covers all cell types. This study is, to our knowledge, the first to cover as many as 5 different cell types, including macrophages, mast cells, neutrophils, eosinophils and basophils. In difference to what some other studies have shown (Woldemeskel *et al.* 2014; Vázquez *et al.* 2021) our results did not reveal any significant increase in infiltration of inflammatory cells in the lymphoma lymph node tumors. A very small increase in neutrophil numbers was noted in the reactive control lymph nodes (compared to the lymphomas which did not have any neutrophils at all), something that might align with the fight against an infection (Valli *et al.* 2016). The differences in the results may be due to several factors, for example the choice of control tissue. Reactive lymph nodes were chosen in this study since locating normal non-reactive lymph nodes in the pathology archive proved challenging. Differences may also be due to slight variations in the protocols and methods; for example, we chose not to count inflammatory cells in the peripheral fat surrounding the lymph nodes since some lymph nodes had much peripheral fat included in the sections and some had none, which would have made an uneven comparison. In this study, only cells inside the capsule was counted. Mast cells, for example, were often seen in peripheral fat, and inclusion of these might have changed the result. Furthermore, the number of both cases and controls included in this study was limited, and the quality of the tissues varied, something that could affect the reliability of the results.

It can be argued that manual counting of cells is an inaccurate method prone to human error. It is a method that relies on the skills and experience of the person conducting it, in this case a student. With that said, all the counting was performed by one and the same person, so the potential source of error would at least have been equal throughout. Furthermore, in all the cell types apart from macrophages, the numbers were so limited that every individual cell could be counted. Con-

versely, the macrophages were so abundant and unevenly distributed that individual cells could not be counted. A scale was therefore constructed from 0-5 to estimate the number of cells in percentage (rather than just addressing them as a few, moderate, or many). Every step on the scale illustrated 20%, and this level of accuracy was chosen since the samples could be divided according to it with a relatively high level of confidence. Nevertheless, a more accurate numerical count would have been desirable to discover significant differences that might disappear in such blunt divisions.

When measuring the degree of inflammation in the tumor microenvironment by counting inflammatory cells, lymphoma is a bit special since it is, in fact, an inflammatory cell type itself that has been tumor-transformed. Further, as described in the literature review, lymph nodes consist almost only of lymphocytes, even under normal conditions (Pawlina 2011). In another cancer form in another organ, we would also have counted the lymphocytes to estimate the degree of inflammation; here, we do not know if there is an increased number of lymphocytes (non-tumor transformed) amongst the tumor-transformed ones. Therefore, the amount of lymphocytes was graded in this study mainly to help in classifying it as B or T-lymphoma. The degree of inflammation was instead mainly assessed by the number of other leukocytes (neutrophils, mast cells, macrophages, eosinophils and basophils), where increased numbers of these would have been interpreted as increased inflammation in the tumor microenvironment. Our results, however, showed no significant differences between the lymphomas and the reactive controls.

It is important to remember that inflammation, acute or chronic, can also be measured by looking at several other parameters than those assessed in this study, such as the general appearance of the histological section, other cell types or subtypes, molecules, pathways or RNA expression (Zhao *et al.* 2021). If assessing other parameters, there might be signs of increased inflammation appearing that could very well be significant to the pathogenesis and prognosis for the patients. Another important aspect to consider regarding if inflammation is significant for the pathogenesis or not, is the site where the primary lymphoma tumor first developed. If it developed in the intestines for example, a chronic inflammation due to IBD may be have been part of the pathogenesis (Faye *et al.* 2022), even though that inflammation can not be seen in the examined lymph node.

One thought is that inflammation could be lower in lymphoma lymph nodes, as examined in this study, than in other organs with lymphoma, because lymphocytes normally exist in the lymph nodes. Lymphocytes belong there, and lymph nodes often get enlarged with increased cell numbers even under normal conditions as they react to infections (Valli *et al.* 2016). Hence, there might not be a strong

reaction when these lymphocytes divide uncontrollably. The lymphocytes move freely in little stroma (Pawlina 2011); therefore, when they expand due to tumor transformation, they likely do so without much destruction of normal tissue that could trigger inflammation. However, the inflammatory reaction might be stronger in other organs, and the tumor cells might have to engage more with other cell types there to survive and grow. They should not be there normally, at least not in such large numbers, and it might require more tricks when they have to avoid detection. However, this study did not investigate inflammation in the microenvironment of lymphoma in other organs/tissues; that is something that needs to be investigated in future studies.

Unfortunately, identifying natural killer cells or classifying the subtypes of lymphocytes and macrophages was beyond the scope of this study. When comparing the total number of macrophages and lymphocytes between the groups, there was no significant difference, they were high in both. However, since the controls were reactive, we cannot rule out the possibility of increased numbers due to inflammation in both these groups, since we did not have any non-reactive lymph nodes to compare with. And we cannot rule out that there is a significant difference in subtypes, for example more cytotoxic T-cells and M1 macrophages that are associated with increased inflammation and immune responses, or more T-regs and M2 macrophages that are associated with decreased inflammation, tissue repair and proliferation (Mills 2012). These cell types seem to be amongst the most important ones in the tumor microenvironment when it comes to interactions with the tumor cells and prognosis for the patient (Carbone *et al.* 2014; Pinheiro *et al.* 2014; Munhoz & Postow 2016; Kim *et al.* 2020; Pan *et al.* 2020; Wolf *et al.* 2023). Investigating this further in future studies would be highly interesting, especially with the literature review in mind.

In this study, there were more B-lymphomas than T-lymphomas, seven vs. three, (three lymphomas could not be classified). An initial idea was to compare these as two separate groups, which unfortunately was not possible since only three turned out to be T-lymphomas. This was slightly disappointing since a lot of resources and time had gone into their classification. When first planning this study, we believed that the lymphomas in the archive would already be classified, which they were not, for this reason it was not possible to pick half B and half T lymphomas. Regarding the method, some issues were initially encountered in the immunohistochemistry, regarding B and T classification, with antibodies that had expired in date and deparaffinization and rehydration liquids being saturated and not freshly changed. These issues were sorted out and the method was re-performed. However, three lymph nodes could still not be classified due to poor staining with CD3 (T) and CD20 (B). The reason for this is unknown. It could be due to autolytic changes,

human errors, or non-B- non-T-lymphomas. If these three had been T-lymphomas, we would have been able to compare the groups of B-lymphomas and T-lymphomas against each other using statistics.

5.2 Serglycin levels

Performing the serglycin quantification with qPCR proved slightly challenging with the formalin-fixed and paraffin-embedded samples. They were of various ages and qualities; and the desirable value 2 in the RNA amount- and quality measurement was not reached in any of the samples. However, the quality value was still fairly close and regarded as *good enough*. It was expected considering the circumstances, namely that the tissue was FFPE, autopsy material with varying degrees of autolytic changes and had been stored for up to 6 years in archive boxes. However, the qPCR did not work well on all the samples. Three samples did not work at all, neither on serglycin nor RPS5; despite a re-performance on the qPCR step with samples from our cDNA library that had been saved in the freezer. While the results still gave a statistical significance, these samples that did not work should ideally be redone from the start to try to achieve values from each, since the number of cases was already limited in this study. One might speculate as to what led to these samples not working in the qPCR, for example if it could be connected to the number of slices put in the tube before the RNA extraction. Since some lymph nodes were very small and others bigger, we added several slices of the smaller ones to get more lymph tissue, not considering that this would also increase the amount of paraffin in the tubes. This might have called for additional Xylene washes. As noted in the lab journal, there were some issues with making the pellets resolve in the tubes, which might support this theory. It can be noted, that two of the samples that did not work at all in the qPCR were also two of the three samples that could not be classified as B or T. When looking at these, the samples are not particularly old, they are all from 2023, and when assessed in the microscope, they might have a varying degree of autolytic changes but do not appear to be worse than any other samples.

So why is the serglycin level significantly lower in the lymphomas while the number of counted inflammatory cells does not differ much? The subtypes of macrophages and T-cells is one aspect that could be different and could explain the serglycin difference since different cell types express different amounts of serglycin (ImmGen.org).

Lymphocytes normally express relatively low serglycin levels, while granulocytes express much more. Since the mutated clones of the tumor transformed lymphocytes are impaired in normal functions, this could explain why serglycin levels are

decreased in the tumor, or, the tumor might have for example fewer cytotoxic T-cells or mast cells. Since we did not type the different subtypes of the T-cells, we do not know the distribution of these. For example, if there are more T-reg or T-helpers, which the tumor might prefer and stimulate differentiation of (Kim *et al.* 2020), there could be fewer cytotoxic T-cells and thereby less serglycin. The mast cells in the peripheral that we chose not to count in this study would have been included in the serglycin measurement since the whole sections of the paraffin blocked lymph nodes were put in the tubes, including the surrounding fat that some of the lymph nodes had. While the mast cells inside the lymph nodes were not significantly different, the mast cells in the peripheral fat could have been different between the groups and resulted in higher serglycin levels in the reactive controls.

Similarly to the discussion regarding the inflammation in lymphoma lymph nodes, one thought here is that lymphocytes, that normally circulate in the bloodstream, might not need serglycin for metastasis in the same manner as other cancer cell types, which do not normally circulate in the blood.

This study has provided a first insight in serglycin levels in canine lymphoma. In contrast to several other studies, in dogs and mice, where tumor tissue and metastatic potential was connected to increased serglycin levels (Roy *et al.* 2016; Jönsson 2019; O'Shee I Sánchez 2021; Djerf 2022; Linder 2022), serglycin levels were decrease in this study, despite almost all cases having metastases in multiple organs. This might be more in line with a study on human breast cancer (Hosoya *et al.* 2022), where low serglycin levels were connected to shorter survival time. This raises questions of why, in some cancer forms, serglycin is increased, and in some, it is not. To further investigate serglycin in canine lymphoma, serglycin levels could be measured in other organs with lymphoma, to see if, for example, the cells start to express higher levels after arrival to a new site where it aims to metastasize. This knowledge would not only help in understanding the use of serglycin as a molecule but also the pathogenesis of the disease. Also, future studies could include a new method known as single-cell RNA sequencing, which enables classification of all cells in the tissue of interest on the transcriptome level (Khozyainova *et al.* 2023). Hence, this would be interesting both regarding the possible infiltration of inflammatory cells and the serglycin expression.

6. Conclusions

In conclusion, in this study, with the methods used, there were no clear indications of increased inflammation in the lymphoma lymph nodes, when reactive lymph nodes were used as controls. The numbers of eosinophils, mast cells, basophils and neutrophils were low in both groups, while macrophages were high in both. Serglycin expression was significantly decreased while almost all cases had metastases in other organs. The reason for the low serglycin is still unknown and needs to be investigated in future studies. The number of mitoses was significantly higher in lymphomas. When cross correlating all the data between inflammatory cells, serglycin and mitoses, the only tendency to a correlation was between increased number of mitoses and decreased serglycin expression.

References

- Bergman, P.J. (2019). Cancer immunotherapies. *The Veterinary Clinics of North America. Small Animal Practice*, 49 (5), 881–902. <https://doi.org/10.1016/j.cvsm.2019.04.010>
- Boes, K.M. & Durham, A.C. (2017). Chapter 13 - Bone marrow, blood cells, and the lymphoid/lymphatic system. In: Zachary, J.F. (ed.) *Pathologic Basis of Veterinary Disease*. 6th ed. Mosby. 724-804.e2. <https://doi.org/10.1016/B978-0-323-35775-3.00013-8>
- Breen, M. & Cullen, J.M. (2020). Chapter 1 - An overview of molecular cancer pathogenesis, and diagnosis. In: *Tumors in Domestic Animals*. John Wiley & Sons, Incorporated. 1–26. <http://ebookcentral.proquest.com/lib/slub-ebooks/detail.action?docID=4737344> [2023-08-29]
- Buchbinder, E.I. & Desai, A. (2016). CTLA-4 and PD-1 pathways: Similarities, differences, and implications of their inhibition. *American Journal of Clinical Oncology*, 39 (1), 98. <https://doi.org/10.1097/COC.0000000000000239>
- Burger, J.A., Ghia, P., Rosenwald, A. & Caligaris-Cappio, F. (2009). The microenvironment in mature B-cell malignancies: a target for new treatment strategies. *Blood*, 114 (16), 3367–3375. <https://doi.org/10.1182/blood-2009-06-225326>
- Carbone, A., Tripodo, C., Carlo-Stella, C., Santoro, A. & Gloghini, A. (2014). The role of inflammation in lymphoma. In: Aggarwal, B.B., Sung, B., & Gupta, S.C. (eds.) *Inflammation and Cancer*. Springer. 315–333. https://doi.org/10.1007/978-3-0348-0837-8_12
- Carmeliet, P. & Jain, R.K. (2000). Angiogenesis in cancer and other diseases. *Nature*, 407 (6801), 249–257. <https://doi.org/10.1038/35025220>
- Chen, L., Deng, H., Cui, H., Fang, J., Zuo, Z., Deng, J., Li, Y., Wang, X. & Zhao, L. (2017). Inflammatory responses and inflammation-associated diseases in organs. *Oncotarget*, 9 (6), 7204–7218. <https://doi.org/10.18632/oncotarget.23208>
- Cho, J. (2022). Basic immunohistochemistry for lymphoma diagnosis. *Blood Research*, 57 (Suppl 1), 55–61. <https://doi.org/10.5045/br.2022.2022037>
- Chun, R., Garrett, L.D. & Vail, D.M. (2000). Evaluation of a high-dose chemotherapy protocol with no maintenance therapy for dogs with lymphoma. *Journal of Veterinary*

Internal Medicine, 14 (2), 120–124. <https://doi.org/10.1111/j.1939-1676.2000.tb02224.x>

- Dagher, O.K., Schwab, R.D., Brookens, S.K. & Posey, A.D. (2023). Advances in cancer immunotherapies. *Cell*, 186 (8), 1814-1814.e1. <https://doi.org/10.1016/j.cell.2023.02.039>
- Djerf, S. (2022). *Mastocytom hos hund - utvärdering av mutationer i c-kit, eosinofilgradering samt genuttryck som potentiella biomarkörer*. [Independent project]. Swedish University of Agricultural Sciences. Veterinary Medicine Programme. <http://urn.kb.se/resolve?urn=urn:nbn:se:slu:epsilon-s-17550>
- Faye, A.S., Holmer, A.K. & Axelrad, J.E. (2022). Cancer in inflammatory bowel disease. *Gastroenterology Clinics of North America*, 51 (3), 649–666. <https://doi.org/10.1016/j.gtc.2022.05.003>
- Flood-Knapik, K.E., Durham, A.C., Gregor, T.P., Sánchez, M.D., Durney, M.E. & Sorenmo, K.U. (2013). Clinical, histopathological and immunohistochemical characterization of canine indolent lymphoma. *Veterinary and Comparative Oncology*, 11 (4), 272–286. <https://doi.org/10.1111/j.1476-5829.2011.00317.x>
- Frantz, A.M., Sarver, A.L., Ito, D., Phang, T.L., Karimpour-Fard, A., Scott, M.C., Valli, V.E.O., Lindblad-Toh, K., Burgess, K.E., Husbands, B.D., Henson, M.S., Borgatti, A., Kisseberth, W.C., Hunter, L.E., Breen, M., O'Brien, T.D. & Modiano, J.F. (2013). Molecular profiling reveals prognostically significant subtypes of canine lymphoma. *Veterinary Pathology*, 50 (4), 693–703. <https://doi.org/10.1177/0300985812465325>
- Guo, J.-Y., Chiu, C.-H., Wang, M.-J., Li, F.-A. & Chen, J.-Y. (2020). Proteoglycan serglycin promotes non-small cell lung cancer cell migration through the interaction of its glycosaminoglycans with CD44. *Journal of Biomedical Science*, 27 (1), 2. <https://doi.org/10.1186/s12929-019-0600-3>
- He, L., Zhou, X., Qu, C., Tang, Y., Zhang, Q. & Hong, J. (2013). Serglycin (SRGN) overexpression predicts poor prognosis in hepatocellular carcinoma patients. *Medical Oncology (Northwood, London, England)*, 30 (4), 707. <https://doi.org/10.1007/s12032-013-0707-4>
- Hosoya, K., Nosaka, K., Sakabe, T., Wakahara, M., Oshima, Y., Suzuki, Y., Nakamura, H. & Umekita, Y. (2022). Clinical significance of serglycin expression in human breast cancer patients. *Anticancer Research*, 42 (1), 279–285. <https://doi.org/10.21873/anticancer.15483>
- Jönsson, L. (2019). *Serglycin, en prognostisk biomarkör för aggressiv cancer i hund*. [Independent project]. Swedish University of Agricultural Sciences. Veterinary Medicine Programme. <http://urn.kb.se/resolve?urn=urn:nbn:se:slu:epsilon-s-10601>
- Kay, J., Thadhani, E., Samson, L. & Engelward, B. (2019). Inflammation-induced DNA damage, mutations and cancer. *DNA Repair*, 83, 102673. <https://doi.org/10.1016/j.dnarep.2019.102673>

- Keller, S.M., Vernau, W., Hodges, J., Kass, P.H., Vilches-Moure, J.G., McElliot, V. & Moore, P.F. (2013). Hepatosplenic and hepatocytotropic T-cell lymphoma: Two distinct types of T-cell lymphoma in dogs. *Veterinary Pathology*, 50 (2), 281–290. <https://doi.org/10.1177/0300985812451625>
- Khozyainova, A.A., Valyaeva, A.A., Arbatsky, M.S., Isaev, S.V., Iamshchikov, P.S., Volchkov, E.V., Sabirov, M.S., Zainullina, V.R., Chechekhin, V.I., Vorobev, R.S., Menyailo, M.E., Tyurin-Kuzmin, P.A. & Denisov, E.V. (2023). Complex analysis of single-cell RNA sequencing data. *Biochemistry. Biokhimiia*, 88 (2), 231–252. <https://doi.org/10.1134/S0006297923020074>
- Kim, J.-H., Kim, B.S. & Lee, S.-K. (2020). Regulatory T cells in tumor microenvironment and approach for anticancer immunotherapy. *Immune Network*, 20 (1), e4. <https://doi.org/10.4110/in.2020.20.e4>
- Kolset, S.O. & Tveit, H. (2008). Serglycin – Structure and biology. *Cellular and Molecular Life Sciences*, 65 (7), 1073–1085. <https://doi.org/10.1007/s00018-007-7455-6>
- Li, X.-J., Ong, C.K., Cao, Y., Xiang, Y.-Q., Shao, J.-Y., Ooi, A., Peng, L.-X., Lu, W.-H., Zhang, Z., Petillo, D., Qin, L., Bao, Y.-N., Zheng, F.-J., Chia, C.S., Iyer, N.G., Kang, T.-B., Zeng, Y.-X., Soo, K.C., Trent, J.M., Teh, B.T. & Qian, C.-N. (2011). Serglycin is a theranostic target in nasopharyngeal carcinoma that promotes metastasis. *Cancer Research*, 71 (8), 3162–3172. <https://doi.org/10.1158/0008-5472.CAN-10-3557>
- Linder, C. (2022). *Serglycin as a potential diagnostic biomarker for hemangiosarcoma in dogs*. [Independent project]. Swedish University of Agricultural Sciences. Veterinary Medicine Programme. <http://urn.kb.se/resolve?urn=urn:nbn:se:slu:epsilon-s-17749>
- Lv, B., Gao, G., Guo, Y., Zhang, Z., Liu, R., Dai, Z., Ju, C., Liang, Y., Tang, X., Tang, M. & Lv, X.-B. (2021). Serglycin promotes proliferation, migration, and invasion via the JAK/STAT signaling pathway in osteosarcoma. *Aging*, 13 (17), 21142–21154. <https://doi.org/10.18632/aging.203392>
- Meuten, D.J., Bienzle, Dorothee & Valli, Victor E. (2020). Chapter 7 - Tumors of the hemolymphatic system. In: *Tumors in Domestic Animals*. John Wiley & Sons, Incorporated. 203–321. <http://ebookcentral.proquest.com/lib/slub-ebooks/detail.action?docID=4737344> [2023-08-30]
- Mills, C.D. (2012). M1 and M2 macrophages: Oracles of health and disease. *Critical Reviews in Immunology*, 32 (6), 463–488. <https://doi.org/10.1615/critrevimmunol.v32.i6.10>
- Munhoz, R.R. & Postow, M.A. (2016). Recent advances in understanding antitumor immunity. *F1000Research*, 5, 2545. <https://doi.org/10.12688/f1000research.9356.1>
- Nelson, R.W. & Couto, C.G. (2020a). Chapter 75 - Principals of cancer treatment. In: *Small Animal Internal Medicine*. 6th ed. Elsevier/Mosby. 1265–1268.
- Nelson, R.W. & Couto, C.G. (2020b). Chapter 79 - Lymphoma. In: *Small Animal Internal Medicine*. 6th ed. Elsevier/Mosby.

- Newkirk, K.M., Brannick, E.M. & Kusewitt, D.F. (2017). Chapter 6 - Neoplasia and tumor biology. In: Zachary, J.F. (ed.) *Pathologic Basis of Veterinary Disease*. 6th ed. Mosby. 286-321.e1. <https://doi.org/10.1016/B978-0-323-35775-3.00006-0>
- O'Shee I Sanchez; E. (2021). *Serglycin expression as a prognosis biomarker in canine mammary tumours*. [Independent project in biology]. Swedish University of Agricultural Sciences. Independent course.
- Ozaki, K., Yamagami, T., Nomura, K. & Narama, I. (2006). T-Cell lymphoma with eosinophilic infiltration involving the intestinal tract in 11 Dogs. *Veterinary Pathology*, 43 (3), 339–344. <https://doi.org/10.1354/vp.43-3-339>
- Pan, Y., Yu, Y., Wang, X. & Zhang, T. (2020). Tumor-associated macrophages in tumor immunity. *Frontiers in Immunology*, 11. <https://www.frontiersin.org/articles/10.3389/fimmu.2020.583084> [2023-10-25]
- Pawlina, W. (2011). Chapter 14 - Lymphatic system, lymphatic tissues and organs. In: *Histology: A Text and Atlas : with Correlated Cell and Molecular Biology*. 6th ed.; International edition. Wolters Kluwer Health. 453–474.
- Pinheiro, D., Chang, Y.-M., Bryant, H., Szladovits, B., Dalessandri, T., Davison, L.J., Yallop, E., Mills, E., Leo, C., Lara, A., Stell, A., Polton, G. & Garden, O.A. (2014). Dissecting the regulatory microenvironment of a large animal model of non-hodgkin lymphoma: Evidence of a negative prognostic impact of FOXP3+ T cells in canine B cell lymphoma. *PLoS ONE*, 9 (8), e105027. <https://doi.org/10.1371/journal.pone.0105027>
- Purushothaman, A., Bandari, S.K., Chandrashekar, D.S., Jones, R.J., Lee, H.C., Weber, D.M. & Orłowski, R.Z. (2017). Chondroitin sulfate proteoglycan serglycin influences protein cargo loading and functions of tumor-derived exosomes. *Oncotarget*, 8 (43), 73723–73732. <https://doi.org/10.18632/oncotarget.20564>
- Rimpo, K., Hirabayashi, M. & Tanaka, A. (2022). Lymphoma in Miniature Dachshunds: A retrospective multicenter study of 108 cases (2006-2018) in Japan. *Journal of Veterinary Internal Medicine*, 36 (4), 1390–1397. <https://doi.org/10.1111/jvim.16455>
- Roy, A., Femel, J., Huijbers, E.J.M., Spillmann, D., Larsson, E., Ringvall, M., Olsson, A.-K. & Åbrink, M. (2016). Targeting serglycin prevents metastasis in murine mammary carcinoma. *PLoS ONE*, 11 (5), e0156151. <https://doi.org/10.1371/journal.pone.0156151>
- Seelig, D.M., Avery, A.C., Ehrhart, E.J. & Linden, M.A. (2016). The comparative diagnostic features of canine and human lymphoma. *Veterinary Sciences*, 3 (2), 11. <https://doi.org/10.3390/vetsci3020011>
- Sutton, V.R., Brennan, A.J., Ellis, S., Danne, J., Thia, K., Jenkins, M.R., Voskoboinik, I., Pejler, G., Johnstone, R.W., Andrews, D.M. & Trapani, J.A. (2016). Serglycin determines secretory granule repertoire and regulates natural killer cell and cytotoxic T lymphocyte cytotoxicity. *The FEBS Journal*, 283 (5), 947–961. <https://doi.org/10.1111/febs.13649>

- Thomas, J.S. (2008). Chapter 69 - Diseases of lymph nodes and lymphatics. In: Morgan, R.V. (ed.) *Handbook of Small Animal Practice*. 5th ed. W.B. Saunders. 690–700.
<https://doi.org/10.1016/B978-1-4160-3949-5.50073-X>
- Toyama-Sorimachi, N., Sorimachi, H., Tobita, Y., Kitamura, F., Yagita, H., Suzuki, K. & Miyasaka, M. (1995). A novel ligand for CD44 is serglycin, a hematopoietic cell lineage-specific proteoglycan: Possible involvement in lymphoid cell adherence and activation. *Journal of Biological Chemistry*, 270 (13), 7437–7444.
<https://doi.org/10.1074/jbc.270.13.7437>
- Vail, D.M., Thamm, D.H. & Liptak, J.M. (2019). Chapter 33 - Hematopoietic tumors. In: *Withrow and MacEwen's Small Animal Clinical Oncology*, 688–772.
<https://doi.org/10.1016/B978-0-323-59496-7.00033-5>
- Valli, V.E., Kass, P.H., Myint, M.S. & Scott, F. (2013). Canine lymphomas: association of classification type, disease stage, tumor subtype, mitotic rate, and treatment with survival. *Veterinary Pathology*, 50 (5), 738–748.
<https://doi.org/10.1177/0300985813478210>
- Valli, V.E.O. (Ted), Kiupel, M., Bienzle, D. & Wood, R.D. (2016). Chapter 2 - Hematopoietic system. In: Maxie, M.G. (ed.) *Jubb, Kennedy & Palmer's Pathology of Domestic Animals: Volume 3*. 6th ed. W.B. Saunders. 102-268.e1.
<https://doi.org/10.1016/B978-0-7020-5319-1.00013-X>
- Vázquez, S., Vallejo, R., Espinosa, J., Arteché, N., Vega, J.A. & Pérez, V. (2021). Immunohistochemical characterization of tumor-associated macrophages in canine lymphomas. *Animals*, 11 (8), 2301. <https://doi.org/10.3390/ani11082301>
- Veluvolu, S., Pellin, M. & Vos, N. (2021). Evaluation of neutrophilia as a prognostic factor in dogs with multicentric lymphoma treated with a cyclophosphamide, doxorubicin, vincristine, and prednisone–based chemotherapy protocol. *Journal of the American Veterinary Medical Association*, 259 (5), 494–502.
<https://doi.org/10.2460/javma.259.5.494>
- Wherry, E.J. (2011). T cell exhaustion. *Nature Immunology*, 12 (6), 492–499.
<https://doi.org/10.1038/ni.2035>
- Woldemeskel, M., Mann, E. & Whittington, L. (2014). Tumor microvessel density–associated mast cells in canine nodal lymphoma. *SAGE Open Medicine*, 2, 2050312114559575. <https://doi.org/10.1177/2050312114559575>
- Wolf, N.K., Kissiov, D.U. & Raulet, D.H. (2023). Roles of natural killer cells in immunity to cancer, and applications to immunotherapy. *Nature Reviews Immunology*, 23 (2), 90–105. <https://doi.org/10.1038/s41577-022-00732-1>
- Zandvliet, M. (2016). Canine lymphoma: a review. *Veterinary Quarterly*, 36 (2), 76–104.
<https://doi.org/10.1080/01652176.2016.1152633>
- Zhao, H., Wu, L., Yan, G., Chen, Y., Zhou, M., Wu, Y. & Li, Y. (2021). Inflammation and tumor progression: signaling pathways and targeted intervention. *Signal*

Transduction and Targeted Therapy, 6 (1), 1–46. <https://doi.org/10.1038/s41392-021-00658-5>

Popular science summary

Does inflammation play a part in cancer? What happens inside a tumor? Lymph node tumors in dog lymphoma

The immune system is getting more and more attention in cancer research, with discoveries leading to new cancer immunotherapies and Nobel prizes in human medicine. Even in our dogs, where cancer is known as one of the most deadly diseases, we are beginning to investigate the immunological aspect, giving new hope for dogs with cancer.

In recent years, science has shown that the problem with cancer may not only be the tumor cells themselves, as they divide uncontrolled and cause organ dysfunction due to replacement of normal tissue or obstructions, but part of the problem could also be our own immune system. Sometimes, our immune cells seem to help the tumor grow and even spread to other parts of the body. When scientists looked closer into the immediate area surrounding the tumor, the so-called *tumor microenvironment*, something astonishing was discovered: In several cancer forms, there is some degree of inflammation. The inflammation is characterized by different immune cells and inflammatory molecules. Also, it was found that, in contrast to what was previously believed, the cells in the immune system can detect and kill cancer cells. This raised an important question: If immune cells can find and kill cancer cells, why do they not beat the tumor? Then, another shivering thing was discovered, namely that cancer cells can interact with immune cells and turn them off by hacking the body's control system. It seems like some immune cells are even lured to the site and stimulated by the tumor to act in ways that help the tumor. The question has also arisen if some immune cells may boost the cancer cells to divide. Much of this remains unknown, especially in dogs and other animals. However, there are connections between what cell types and how many of them are present in the *tumor microenvironment* and the survival time for the patient.

In our study, we wanted to examine degree of inflammation in dog tumors by looking at the infiltration of inflammatory cells. We picked a tumor type called lymphoma, which is a tumor that can be seen in lymph nodes but also in other organs. In the lymphoma we also wanted to measure the levels of the molecule

serglycin, since serglycin has been closely associated with the tumors' ability to metastasize in previous studies on other cancer forms. By studying what happens in the tumor microenvironment of this cancer type on cell and molecule level, we wanted to understand more about how the disease works. These types of details could possibly also be used in the future to design diagnostic methods, predict prognosis for patients, or even develop new treatments that can help give our dogs with cancer a longer survival time, or a higher quality of life in the time they have left.

The results of our study showed that in this cancer type in dogs, there is probably very little inflammation or involvement of inflammatory cells in the tumors, apart from the tumor cells themselves and the immune cells that already belong in the lymph nodes (lymphocytes and macrophages). Therefore, it would be interesting to investigate these particular cell types in more detail, for example their subtypes (our study did not include this since we would have needed more resources and time). The lymphocytes and macrophage may change their subtype in a tumor, in other words their character and molecule production, affecting the tumor's growth and the patient's survival time.

An interesting discovery in this study was that serglycin was lower in the tumors than in the controls. In other studies, this molecule has been increased and associated with higher malignancy and metastasis; in mouse breast cancer, the lack of this molecule prevented the spread of the cancer. Since almost all of our cases of lymphoma metastasizes to multiple organs, we expected serglycin to be increased in the lymph nodes, which it was not. The low levels should be confirmed with more studies, but if they are true, this is valuable new knowledge. For example, imagine the following scenario: If serglycin had been used as a biomarker to detect cancer in patients in the future, or as a target in cancer treatment. Then lymphoma in the lymph nodes might have been missed without having this information, giving a false security that could prolong detection and proper treatment. The reason why the serglycin levels were low in the lymphomas in this study, however, is still unknown, and needs to be investigated further in future studies.

Acknowledgements

This study would not have been possible without the financial funding from Elsa Paulssons Foundation Memorial Scholarship, we sincerely thank you for supporting and believing in this exciting project.

I would like to sincerely thank my supervisor, Magnus Åbrink (associate professor and senior lecturer in immunology) for all the kindness, support, encouragement, and inspiration during this project.

Also, I would like to say a special thanks to Albin Norman and Vidar Skullerud, biomedical analytics in the history lab, for all the help and support, and for teaching me all I needed to know about histological work, from preparation to staining and immunohistochemistry.

Furthermore, I would like to thank my assistant supervisor, Fredrik Södersten, senior pathologist, for helping me assess the tissues and stainings, which has been very valuable to me in this project.

I also want to express my gratitude to Karin Vargmar, my examiner, who helped me in various ways, giving valuable inputs and helping me to localize educational material that facilitated the process.

In addition, I wish to thank the whole pathology team at BVF for letting me participate in various events surrounding their work, for showing interest in my project, and for attempting to help and support me whenever they could.

I thank Bernt Hjertner for guidance in the lab with routines, security, and the qPCR machine.

Last but not least, I want to Thank my work group for this fall; it has been fun and rewarding to share this project experience with you, to catch up on our weekly meetings, and to follow the progress of your interesting respective projects.

Appendix 1

Regular histological stainings: Hematoxylin-Eosin HE

Materials

Mayer's hematoxylin (purchased ready to use)

Eosin Y 0,2 % (purchased, 1 mL HAc/ca 200 mL added)

Execution

- Incubate the slices in 60 C, 40 minutes.
- Rehydration:
 - Xylen I, 15 minutes.
 - Xylen II, 15 minutes.
 - ABS I, 5 minutes.
 - ABS II, 5 minutes.
 - 95 % alc., 5 minutes.
 - 70 % alc., 5 minutes.
- Rinse in tapwater, 5 minutes.
- Mayer's hematoxylin, 5 minutes.
- Rinse in tapwater, 20 minutes.
- Eosin, 30-60 seconds.
- Dehydration:
 - 95 % alc., splash shortly.
 - 95 % alc., splash shortly.
 - ABS I, 2 minutes.
 - ABS II, 2 minutes.
 - ABS III, 5 minutes.
 - Xylen I, splash.
 - Xylen II, splash.
 - Xylen III, 2+ minutes.
- Installation of cover glasses with Pertex.

Results

Nucleus stain blue, connective tissue, erythrocytes and cytoplasm stain red, pink and orange.

Appendix 2

Regular histological stainings: Giemsa

Materials

2 % Giemsa (purchased ready to use, then diluted to 1:50)

Execution

- Incubate the slices in 60 C, 40 minutes.
- Rehydration:
 - Xylen I, 15 minutes
 - Xylen II, 15 minutes
 - ABS I, 5 minutes
 - ABS II, 5 minutes
 - 95 % alc., 5 minutes
 - 70 % alc., 5 minutes
- Splash in deionised water
- 2 % Giemsa, 30 minutes
- Rinse in deionised water
- Splash in 70 % etanol
- Dehydration:
 - 95 % alc., splash shortly.
 - 95 % alc., splash shortly.
 - ABS I, 2 minutes.
 - ABS II, 2 minutes.
 - ABS III, 5 minutes.
 - Xylen I, splash.
 - Xylen II, splash.
 - Xylen III, 2+ minutes.
- Installation of cover glasses with Pertex.

Results

Background will be varying shades of blue. Erythrocytes will be weekly orange red, Nucleus will be blue. Mast cells will have strong purple stained granula. Helicobacter will be dark blue and spiral shaped.

Appendix 3

Regular histological stainings: Tolluedine blue

Material

0,5 % Toluidine blue i 20 % alcohol (purchased ready to use, has to be filtrated)

Utförande

- Incubate the slices in 60 C, 40 minutes.
- Rehydration:
 - Xylen I, 15 minutes
 - Xylen II, 15 minutes
 - ABS I, 5 minutes
 - ABS II, 5 minutes
 - 95 % alk., 5 minutes
 - 70 % alk., 5 minutes
 - Deionised water
- Toluidine blue, 20 minutes
- 95 % alcohol x 2, splash (until excess staining has been washed off)
- Dehydration:
 - 95 % alc., splash shortly.
 - ABS I, splash shortly.
 - ABS II, 2 minutes
 - ABS III, 5 minutes
 - Xylen I, splash.
 - Xylen II, splash.
 - Xylen III, 2+ minutes
- Installation of cover glasses with Pertex.

Results

Mast cells will be stained strongly blue/viol.

.

Appendix 4

Immunohistochemistry: CD3

Materials

	<i>Dilution</i>	<i>Art. nr.</i>	<i>Lot nr.</i>	<i>Protein conc.</i>
TBS, pH 7.6	1:10	-	-	-
Tris-EDTA, pH 9		-	-	-
30 % H ₂ O ₂	1:10	1.07209.0250	K52822909040	-
Anti-CD3	1:50	M7051	20043699	138 mg/L
Mouse IgG1	1:36	X0931	20084260	100 mg/L
Normal Goat Serum	1:50	X0907	20078389	100 g/L
EnVision Anti-Mouse		K4001	11092987	-
DAB+ Chromogen		K3468	11246742	-

Principal

The antibody marks CD3 ϵ and is a useful tool in identification of T-cells and associated neoplasms.

Execution

- Incubate the slices in 60 C, for 40 minutes.
- Rehydration:
 - Xylen I, 15 minutes
 - Xylen II, 15 minutes
 - ABS I, 5 minutes
 - ABS II, 5 minutes
 - 95 % alc., 5 minutes
 - 70 % alc., 5 minutes
- Deionised water x3
- Antigen retrieval in Tris-EDTA pH 9, 95°C with Decloaking Chamber, 20 minutes.
- Rinse in deionised water x3.
- Block endogenous peroxidase with 3 % hydrogen peroxide (H₂O₂) for 5 minutes in darkness and room temperature.

- Rinse carefully in deionised water.
- Rinse in TBS x3.
- Mark with fat pen around the sections.
- Block unspecific binding with Normal goat serum 1:50, 30 min room temperature.
- Drain the slices.
- Incubate the slices with primary antibody (CD3) and isotype control, 30 minutes, room temperature.
- Rinse in TBS x3.
- Incubate the sections with EnVision (directly from the bottle) 30 minutes, room temperature.
- Rinse in TBS x3.
- Development in DAB-solution, 4 minutes, in darkness, room temperature.
- Rinse in tapwater for 15 minutes.
- Mayers hematoxylin, 1 minute.
- Rinse in tapwater for 15 minutes.
- Dehydrering:
 - 95 % alc., splash shortly
 - 95 % alc., splash
 - ABS I, 2 minutes
 - ABS II, 2 minutes
 - ABS III, 5 minutes
 - Xylen I, splash
 - Xylen II, 1-2 minutes
 - Xylen III, 2+ minutes
- Installation of cover glass with Pertex

Results

T-cells are stained with brown colour in the cytoplasm and or the cell membrane. In the lymph node inter follicular areas containing T-lymphocytes will be stained strongly, as well as small reactive T-cells in the B-cell follicles.

Appendix 5

Immunohistochemistry: CD20

Materials

	<i>Dilution</i>	<i>Art. nr.</i>	<i>Lot nr.</i>	<i>Protein conc.</i>
TBS, pH 7.6	1:10	-	-	-
Tris-EDTA, pH 9		-	-	-
30 % H ₂ O ₂	1:10	1.07209.0250	K52822909040	-
Anti-CD20	1:400	PA5-16701	YG3990461	0,077mg/ml
Rabbit IgG	1:260-1:400	X0931	20084260	20 mg/L
Normal Goat Serum	1:50	X0907	20078389	100 g/L
EnVision Anti-Rabbit		K4003	11092987	-
DAB+ Chromogen		K3468	11246742	-

Principal

The antibody marks B-cells.

Execution

- Incubate the slices in 60 C, 40 minutes.
- Rehydration:
 - Xylen I, 15 minutes
 - Xylen II, 15 minutes
 - ABS I, 5 minutes
 - ABS II, 5 minutes
 - 95 % alc., 5 minutes
 - 70 % alc., 5 minutes
- Deionised water x3.
- Antigen retrieval in Tris-EDTA pH 9, 95°C with Decloaking Chamber, 20 minutes.
- Rinse in deionised water x 3.
- Block endogenous peroxidase with 3 % hydrogen peroxide H₂O₂, 5 minutes in darkness, room temperature.
- Rinse carefully in water.
- Rinse in TBS x3.
- Mark with fat pen around the sections.
- Block unspecific binding with Normal goat serum 1:50, 30 min, room temperature.
- Drain the slices.

- Incubate the sections with primary antibody (CD20) and isotype control antibody, 30 minutes, room temperature.
- Rinse in TBS x3.
- Incubate the sections with EnVision directly from the bottle for 30 minutes, room temperature.
- Rinse in TBS x3.
- Development in DAB solution, 4 minutes in darkness, room temperature.
- Rinse in tapwater, 15 minutes.
- Mayers hematoxylin, 1 minute.
- Rinse in tapwater, 15 minutes.
- Dehydration:
 - 95 % alc., splash shortly.
 - 95 % alc., splash.
 - ABS I, 2 minutes.
 - ABS II, 2 minutes.
 - ABS III, 5 minutes.
 - Xylen I, splash.
 - Xylen II, 1-2 minutes.
 - Xylen III, 2+ minutes.
- Installation of cover glasses with Pertex.

Results

Cells stained with the antibody show brown colouration of the cell membrane and or the cytoplasm. Nucleoli stain blue.

Appendix 6

Immunohistochemistry: Iba-1

Materials

	<i>Dilution</i>	<i>Art. nr.</i>	<i>Lot nr.</i>	<i>Protein conc.</i>
PBS, pH 7.4 (tablet)		09-9400-100	271402-01	-
Na-citrate buffer, pH 6		-	-	-
30 % H ₂ O ₂	1:10	1.07209.0250	K52822909040	-
Anti-Iba1	1:500	019-19741	CAP4688	0,5 mg/mL
Rabbit Normal IgG	1:40-1:500	X0936	20002897	20 g/L
Normal Goat Serum	1:50	X0907	20078389	100 g/L
EnVision Anti-Rabbit		K4003	11337301	-
DAB+ Chromogen		K3468	11246742	-

Principal

The antibody binds the macrophage/microglia specific protein Iba-1 (ionized calcium binding adapter molecule 1) which is a significant part of the cell signaling. The protein is upregulated when these cells are activated.

Execution

- Incubate the slices in 60 C in 40 minutes.
- Rehydration:
 - Xylen I, 15 minutes
 - Xylen II, 15 minutes
 - ABS I, 5 minutes
 - ABS II, 5 minutes
 - 95 % alc., 5 minutes
 - 70 % alc., 5 minutes
- Deionised water x3.
- Antigen retrieval in Na-citrate buffer pH 6, 95°C with Decloaking Chamber, 20 minutes.
- Let it cool for 20 minutes in room temperature.
- Rinse in deionised water x3.
- Block endogenous peroxidase in 3 % hydrogen peroxide H₂O₂ for 5 minutes in darkness, room temperature.
- Rinse carefully in deionised water.
- Rinse in PBS x3 .
- Mark with fat pen around the sections.

- Block unspecific binding with Normal goat serum 1:50, 30 min, room temperature.
- Drain the slices.
- Incubate the sections with primary antibody (Iba-1) and isotype control antibody for 30 min in room temperature.
- Rinse in PBS x3
- Incubate the sections with EnVision directly from the bottle, 30 min, room temperature.
- Rinse in PBS x3.
- Development in DAB solution for 4 minutes in darkness, room temperature.
- Rinse in tapwater, 15 minutes.
- Mayer's hematoxylin, 1 minute.
- Rinse in tapwater, 15 minutes.
- Dehydration:
 - 95 % alc., splash shortly.
 - 95 % alc., splash.
 - ABS I, 2 minutes
 - ABS II, 2 minutes.
 - ABS III, 5 minutes.
 - Xylen I, splash.
 - Xylen II, 1-2 minutes.
 - Xylen III, 2+ minutes.
- Installation of cover glasses with Pertex.

Results

Positive cells get a brown staining, background and nucleoli stain blue.

Appendix 7

Preparing total RNA from FFPE blocks

- Using a microtome cut two (or three slices if smaller amounts of tissues) slices 20 µm thick and transfer to 1,5-ml siliconized tubes
- Incubate the slices twice in 1 ml of xylene at 50°C for 5 minutes, followed by centrifugation at 13,000rpm
- Wash pellets twice in 1 ml of 99,5% ethanol and air-dry at room temperature. (If the pellets were not attached to the tubes surface, it was centrifugated at 13000rpm for 1 minute).
- Incubate the dried pellets in 150 µm of 1X proteinase K digestion buffer (20mmol/L Tris-HCl, pH 8.0; 1mmol/L CaCl₂, 0,5% sodium dodecyl sulfate), containing 400 µm/ml proteinase K at 55°C for 3 hours. Incubate in 95°C for 5 minutes and cool down to room temperature.
- Extract total RNA using the 1 ml TRIzol (Invitrogen, Carlsbad, CA) method according to the manufacturer's instructions (please see appendix 2 for page 1-3 of the manufacturer's instructions). Some adaptations were made based on empirical evidence, and these adaptations are written in the specific step:
 - o Add 0,2 mL of chloroform per 1 mL of TRIzol reagent used for lysis, then securely cap the tube
 - o Incubate for 2-3 minutes. Adaptions: This step was changed. samples were incubated at least 10 minutes to increase the yield, and then the samples were vortexed every 2-3 minutes.
 - o Centrifuge samples 15 minutes at 12,000 x g at 4°C. The mixture separates into a lower red phenol-chloroform, and interphase, and a colorless upper aqueous phase.

- Transfer the aqueous phase containing the RNA to a new tube. Adaption: About 500-600 μm was transferred from each sample.
 - Transfer the aqueous phase containing the RNA to a new tube by angling the tube at 45 °C and pipetting the solution out. IMPORTANT: avoid transferring any of the interphase or organic layer into the pipette when removing the aqueous phase.
- Isolate RNA according to the manufacturer's instructions:
 - Add 0,5 mL of isopropanol to the aqueous phase, per 1 mL of TRIzol reagent used for lysis. Adaption: 500-600 μm of isopropanol was added.
 - Incubate for 10 minutes or more.
 - Centrifuge for 10 minutes at 12,000 x g at 4°C. Total RNA precipitate forms a white gel like pellet at the bottom of the tube.
 - Discard the supernatant with a micropipette.
 - Wash the RNA according to the manufacturer's instructions:
 - Resuspend the pellet in 1 mL of 75% ethanol per 1 mL of TRIzol reagent used for lysis. Adaptions: ethanol of 70% was used instead of 75%. Note: the RNA can be stored in 75 % ethanol for at least 1 year at -20 °C, or at least one week at 4 °C.
 - Vortex the sample briefly, then centrifugate for 5 minutes at 7500 x g at 4°C.
 - Discard the supernatant with a micropipettor.
 - Vacuum or air dry the RNA pellets for 5-10 minutes.
 - 30 μL of nuclease free water was added after air drying, and then incubated in 55°C for 10 minutes.
 - Determine the yield and quality 260/280 optical density (OD) ratios of RNA product by the nano-drop spectrophotometer

Appendix 8

Trizol, manufacturers instructions page 1 - 3

invitrogen

USER GUIDE

TRIZOL™ Reagent

Catalog Numbers 15596026 and 15596018

Doc. Part No. 15596026.PPS Pub. No. MAN0001271 Rev. C.0



WARNING! Read the Safety Data Sheets (SDSs) and follow the handling instructions. Wear appropriate protective eyewear, clothing, and gloves. Safety Data Sheets (SDSs) are available from thermofisher.com/support.

Product description

Invitrogen™ TRIZOL™ Reagent is a ready-to-use reagent, designed to isolate high quality total RNA (as well as DNA and proteins) from cell and tissue samples of human, animal, plant, yeast, or bacterial origin, within one hour. TRIZOL™ Reagent is a monophasic solution of phenol, guanidine isothiocyanate, and other proprietary components which facilitate the isolation of a variety of RNA species of large or small molecular size. TRIZOL™ Reagent maintains the integrity of the RNA due to highly effective inhibition of RNase activity while disrupting cells and dissolving cell components during sample homogenization. TRIZOL™ Reagent allows for simultaneous processing of a large number of samples, and is an improvement to the single-step RNA isolation method.

TRIZOL™ Reagent allows users to perform sequential precipitation of RNA, DNA, and proteins from a single sample. After homogenizing the sample with TRIZOL™ Reagent, chloroform is added, and the homogenate is allowed to separate into a clear upper aqueous layer (containing RNA), an interphase, and a red lower organic layer (containing the DNA and proteins). RNA is precipitated from the aqueous layer with isopropanol. DNA is precipitated from the interphase/organic layer with ethanol. Protein is precipitated from the phenol-ethanol supernatant by isopropanol precipitation. The precipitated RNA, DNA, or protein is washed to remove impurities, and then resuspended for use in downstream applications.

- Isolated RNA can be used in RT-PCR, Northern Blot analysis, Dot Blot hybridization, poly(A)⁺ selection, in vitro translation, RNase protection assay, and molecular cloning.
- Isolated DNA can be used in PCR, Restriction Enzyme digestion, and Southern Blots.
- Isolated protein can be used for Western Blots, recovery of some enzymatic activity, and some immunoprecipitation.

For DNA isolation, see the *TRIZOL™ Reagent (DNA isolation) User Guide* (Pub. No. MAN0016385).

TRIZOL™ Reagent can also be used with Phasemaker™ Tubes (Cat. No. A33248) to isolate RNA. Phasemaker™ Tubes creates a solid barrier between the organic and aqueous phases of the TRIZOL™ Reagent following sample homogenization which makes separation of phases easier. See the *TRIZOL™ Reagent and Phasemaker™ Tubes Complete System User Guide* (Pub. No. MAN0016163) for the full protocol.

TRIZOL™ Reagent can also be used with the PureLink™ RNA Mini Kit (Cat. No. 12183018A) which uses spin columns instead of ethanol precipitation to purify the RNA. For additional information, see the *PureLink™ RNA Mini Kit User Guide* (Pub. No. MAN0000406).

Contents and storage

Contents	Cat. No. 15596026 (100 reactions)	Cat. No. 15596018 (200 reactions)	Storage
TRIZOL™ Reagent	100 mL	200 mL	2–25°C

Required materials not supplied

Unless otherwise indicated, all materials are available through thermofisher.com. "MLS" indicates that the material is available from fisherscientific.com or another major laboratory supplier.

Table 1 Materials required for all isolations

Item	Source
Equipment	
Centrifuge and rotor capable of reaching 12,000 × g and 4°C	MLS
Tubes	
Polypropylene microcentrifuge tubes	MLS
Reagents	
Chloroform	MLS

Table 2 Materials required for RNA isolation

Item	Source
Equipment	
Water bath or heat block at 55–60°C	MLS
Reagents	
Isopropanol	MLS
Ethanol, 75%	MLS
RNase-free water or 0.5% SDS	MLS
(Optional) RNase-free glycogen or 0.1 mM EDTA	MLS

Table 3 Materials required for protein isolation

Item	Source
Equipment	
(Optional) Dialysis membranes	MLS
Reagents	
Isopropanol	MLS
Ethanol, 100%	MLS
0.3 M Guanidine hydrochloride in 95% ethanol	MLS
1% SDS	MLS

Input sample requirements

IMPORTANT! Perform RNA isolation immediately after sample collection or quick-freeze samples immediately after collection and store at –80°C or in liquid nitrogen until RNA isolation.

Sample type	Starting material per 1 ml of TRIZOL reagent
Tissues ^[1]	50–100 mg of tissue
Cells grown in monolayer	1 × 10 ⁵ –1 × 10 ⁷ cells grown in monolayer in a 3.5-cm culture dish (10 cm ²)
Cells grown in suspension	5–10 × 10 ⁶ cells from animal, plant, or yeast origin or 1 × 10 ⁷ cells of bacterial origin

^[1] Fresh tissues or tissues stored in RNAlater™ Stabilization Solution (Cat. No. AM7020).

For Research Use Only. Not for use in diagnostic procedures.

ThermoFisher
SCIENTIFIC

Procedural guidelines

- Perform all steps at room temperature (20–25°C) unless otherwise noted.
- Use cold TRIzol™ Reagent if the starting material contains high levels of RNase, such as spleen or pancreas samples.
- Use disposable, individually wrapped, sterile plasticware and sterile, disposable RNA-free pipettes, pipette tips, and tubes.
- Wear disposable gloves while handling reagents and RNA samples to prevent RNase contamination from the surface of the skin; change gloves frequently, particularly as the protocol progresses from crude extracts to more purified materials.
- Always use proper microbiological aseptic techniques when working with RNA.
- Use RNaseZap™ RNase Decontamination Solution (Cat. no. AM9780) to remove RNase contamination from work surfaces and non-disposable items such as centrifuges and pipettes used during purification.
- Ensure that all materials that come into contact with TRIzol™ Reagent are compatible with phenol, guanidine isothiocyanate, and chloroform.

- Add 1 mL of TRIzol™ Reagent per 0.25 mL of sample (5–10 × 10⁶ cells from animal, plant, or yeast origin or 1 × 10⁷ cells of bacterial origin) to the pellet.

Note: Do not wash cells before addition of TRIzol™ Reagent to avoid mRNA degradation.

- Pipet the lysate up and down several times to homogenize.

Note: The sample volume should not exceed 10% of the volume of TRIzol™ Reagent used for lysis.

STOPPING POINT Samples can be stored at 4°C overnight or at –20°C for up to a year.

2. (Optional) If samples have a high fat content, centrifuge the lysate for 5 minutes at 12,000 × g at 4–10°C, then transfer the clear supernatant to a new tube.
3. Incubate for 5 minutes to allow complete dissociation of the nucleoproteins complex.
4. Add 0.2 mL of chloroform per 1 mL of TRIzol™ Reagent used for lysis, securely cap the tube, then thoroughly mix by shaking.
5. Incubate for 2–3 minutes.
6. Centrifuge the sample for 15 minutes at 12,000 × g at 4°C. The mixture separates into a lower phenol-chloroform, an interphase, and a colorless upper aqueous phase.
7. Transfer the aqueous phase containing the RNA to a new tube by angling the tube at 45° and pipetting the solution out.

IMPORTANT! Avoid transferring any of the interphase or organic layer into the pipette when removing the aqueous phase.

Proceed directly to "Isolate RNA" on page 2.

To isolate DNA or protein, save the interphase and organic phase. See the *TRIzol™ Reagent (DNA isolation) User Guide* (Pub. No. MAN0016385) or see "Isolate proteins" on page 3 for detailed procedures. The organic phase can be stored at 4°C overnight.

Lyse samples and separate phases

1. Lyse and homogenize samples in TRIzol™ Reagent according to your starting material.
 - **Tissues:**

Add 1 mL of TRIzol™ Reagent per 50–100 mg of tissue to the sample and homogenize using a homogenizer.
 - **Cell grown in monolayer:**
 - a. Remove growth media.
 - b. Add 1 mL of TRIzol™ Reagent per 1 × 10⁵–1 × 10⁷ cells directly to the 3.5-cm culture dish to lyse the cells.
 - c. Pipet the lysate up and down several times to homogenize.
 - **Cells grown in suspension:**
 - a. Collect the cells by centrifugation and discard the supernatant.

Isolate RNA

- | | | |
|----------|---------------------|---|
| 1 | Precipitate the RNA | <ol style="list-style-type: none"> 1.1. (Optional) If the starting sample is small (<10⁶ cells or <10 mg of tissue), add 5–10 µg of RNase-free glycogen as a carrier to the aqueous phase. <p>Note: The glycogen is co-precipitated with the RNA, but does not interfere with subsequent applications.</p> 1.2. Add 0.5 mL of isopropanol to the aqueous phase, per 1 mL of TRIzol™ Reagent used for lysis. 1.3. Incubate for 10 minutes at 4°C. 1.4. Centrifuge for 10 minutes at 12,000 × g at 4°C. <p>Total RNA precipitate forms a white gel-like pellet at the bottom of the tube.</p> 1.5. Discard the supernatant with a micropipettor. |
| 2 | Wash the RNA | <ol style="list-style-type: none"> 2.1. Resuspend the pellet in 1 mL of 75% ethanol per 1 mL of TRIzol™ Reagent used for lysis. <p>Note: The RNA can be stored in 75% ethanol for at least 1 year at –20°C, or at least 1 week at 4°C.</p> 2.2. Vortex the sample briefly, then centrifuge for 5 minutes at 7500 × g at 4°C. 2.3. Discard the supernatant with a micropipettor. 2.4. Vacuum or air dry the RNA pellet for 5–10 minutes. <p>IMPORTANT! Do not dry the pellet by vacuum centrifuge. Do not let the RNA pellet dry, to ensure total solubilization of the RNA. Partially dissolved RNA samples have an A_{230/280} ratio <1.6.</p> |
| 3 | Solubilize the RNA | <ol style="list-style-type: none"> 3.1. Resuspend the pellet in 20–50 µL of RNase-free water, 0.1 mM EDTA, or 0.5% SDS solution by pipetting up and down. <p>IMPORTANT! Do not dissolve the RNA in 0.5% SDS if the RNA is to be used in subsequent enzymatic reactions.</p> 3.2. Incubate in a water bath or heat block set at 55–60°C for 10–15 minutes. <p>Proceed to downstream applications, or store the RNA at –70°C.</p> |

4	Determine the RNA yield	Determine the RNA yield using one of the following methods.						
		<table border="1"> <thead> <tr> <th>Method</th> <th>Procedure</th> </tr> </thead> <tbody> <tr> <td> Absorbance Absorbance at 260 nm provides total nucleic acid content, while absorbance at 280 nm determines sample purity. Since free nucleotides, RNA, ssDNA, and dsDNA absorb at 260 nm, they all contribute to the total absorbance of the sample. </td> <td> <ol style="list-style-type: none"> 1. Dilute sample in RNase-free water, then measure absorbance at 260 nm and 280 nm. 2. Calculate the RNA concentration using the formula A₂₆₀ × dilution × 40 = µg RNA/mL. 3. Calculate the A₂₆₀/A₂₈₀ ratio. <p>A ratio of ~2 is considered pure.</p> <p>RNA samples can be quantified by absorbance without prior dilution using the NanoDrop™ Spectrophotometer. Refer to the instruments instructions for more information.</p> </td> </tr> <tr> <td> Fluorescence Fluorescence selectively measures intact RNA, but does not measure protein or other contaminants present in the sample </td> <td> <ul style="list-style-type: none"> • Quantify RNA yield using the appropriate Qubit™ or Quant-IT™ RNA Assay Kit (Cat. Nos. Q32852, Q10210, Q33140, or Q10213). Refer to the kits instructions for more information. </td> </tr> </tbody> </table>	Method	Procedure	Absorbance Absorbance at 260 nm provides total nucleic acid content, while absorbance at 280 nm determines sample purity. Since free nucleotides, RNA, ssDNA, and dsDNA absorb at 260 nm, they all contribute to the total absorbance of the sample.	<ol style="list-style-type: none"> 1. Dilute sample in RNase-free water, then measure absorbance at 260 nm and 280 nm. 2. Calculate the RNA concentration using the formula A₂₆₀ × dilution × 40 = µg RNA/mL. 3. Calculate the A₂₆₀/A₂₈₀ ratio. <p>A ratio of ~2 is considered pure.</p> <p>RNA samples can be quantified by absorbance without prior dilution using the NanoDrop™ Spectrophotometer. Refer to the instruments instructions for more information.</p>	Fluorescence Fluorescence selectively measures intact RNA, but does not measure protein or other contaminants present in the sample	<ul style="list-style-type: none"> • Quantify RNA yield using the appropriate Qubit™ or Quant-IT™ RNA Assay Kit (Cat. Nos. Q32852, Q10210, Q33140, or Q10213). Refer to the kits instructions for more information.
Method	Procedure							
Absorbance Absorbance at 260 nm provides total nucleic acid content, while absorbance at 280 nm determines sample purity. Since free nucleotides, RNA, ssDNA, and dsDNA absorb at 260 nm, they all contribute to the total absorbance of the sample.	<ol style="list-style-type: none"> 1. Dilute sample in RNase-free water, then measure absorbance at 260 nm and 280 nm. 2. Calculate the RNA concentration using the formula A₂₆₀ × dilution × 40 = µg RNA/mL. 3. Calculate the A₂₆₀/A₂₈₀ ratio. <p>A ratio of ~2 is considered pure.</p> <p>RNA samples can be quantified by absorbance without prior dilution using the NanoDrop™ Spectrophotometer. Refer to the instruments instructions for more information.</p>							
Fluorescence Fluorescence selectively measures intact RNA, but does not measure protein or other contaminants present in the sample	<ul style="list-style-type: none"> • Quantify RNA yield using the appropriate Qubit™ or Quant-IT™ RNA Assay Kit (Cat. Nos. Q32852, Q10210, Q33140, or Q10213). Refer to the kits instructions for more information. 							

Appendix 9

cDNA synthesis

Before the cDNA synthesis started the samples were diluted with RNase free water until the same concentration was achieved in all samples. The lowest concentration sample was used as a reference and not diluted.

CLEAN ROOM	
Prepare DNase treatment Mix for each RNA sample	
	V(μ L)
10x xRxn Buffer	1,2
Nuclease free water	$12 - V_{(RNA)} - 1,2 - 1,2$
DNase 1 Invitrogen AMPD1	1,2
Total	$12 - V_{(RNA)}$

TEMPLATE ROOM	
DNase treatment mix for each RNA RT+ sample	
	V (μ l)
RNA	*
DNase treatment Mix	$12 - V_{(RNA)}$
Total	12
Mix gently by pipetting up and down, incubate at room temperature for 15 minutes.	
DNase stop (EDTA)	1,2
Total RNA treated	13,2
Incubate at 70 °C for 10 minutes, chill on ice for about 5 minutes, spine down	

CLEAN ROOM	
Prepare cDNA Master Mix 1	
Number of reactions	1
Primer mix 2uM** (μ l)	1,2
dNTPs mix 10 uM (μ l)	1,2
Total (μ l)	2,4
Primer Mix**: Even V of each (rev SGN, rev GAPDH, rev HPRT, revEEF2, rev RPS5 and Oligo DT)	

TEMPLATE ROOM	
cDNA Master Mix 1 for each RNA	
RNA treated (μ l)	13,2
Master Mix 1 (μ l)	2,4

Total (μl)	15,6
Anneal at 59°C for 5 minutes, put on ice >1 minute.	

CLEAN ROOM		
Prepare cDNA Master Mix 2		
	RT+	RT-
Number of reactions	1	1
5x First-Strand Buffer (μl)	4	0,8
0,1M DTT (μl)	1	0,2
Superscript 4 RT (200U/ul) (μl)	1	0
Nuclease free water (μl)	1	0,4
Total (μl)	7	1,4

TEMPLATE ROOM		
cDNA Master Mix 2 for each reaction		
	RT+	RT-
Master Mix 2 (μl)	7	1,4
Template RNA treated (μl)	13	2,6
Total (μl)	20	4
Incubate at 25 °C for 15 minutes		
Incubate at 55 °C for 60 minutes		
Inactive reaction at 70 °C for 15 minutes		

Appendix 10

Master Mix and qPCR protocol

Samples: 1:5 dilution with RNase free water
Vessel: Bio-Rad white plate
Seal: Bio-Rad optical seal
Primerstock, uM: 10
Primerconc (final uM): 0,4
Replicates: 2

Prepare the master mixes according to the table for the given amount of reactions and for the specific gene:

CLEAN ROOM	
Preparation qPCR mix	
Per number of reactions	1
	V(μ L)
SYBRGreen master mix	12,5
Primer forward	1
Primer reverse	1
Nuclease free water	8,5
Total μl mastermix per well	23

Template room:

- Add μ l mastermix per well: 23
- Add μ l sample per well: 2

Program

1. 95 °C for 5 min
2. 95 °C for 15 sec
3. 58 °C for 30 sec
4. 72 °C for 30 sec, collect SYBR green
5. Go to step 2, 39 times
6. Melt curve: 60 °C, 0,5 °C steps to 95 °C, 10 sec dwell time

Publishing and archiving

Approved students' theses at SLU are published electronically. As a student, you have the copyright to your own work and need to approve the electronic publishing. If you check the box for **YES**, the full text (pdf file) and metadata will be visible and searchable online. If you check the box for **NO**, only the metadata and the abstract will be visible and searchable online. Nevertheless, when the document is uploaded it will still be archived as a digital file. If you are more than one author, the checked box will be applied to all authors. Read about SLU's publishing agreement here:

- <https://www.slu.se/en/subweb/library/publish-and-analyse/register-and-publish/agreement-for-publishing/>.

YES, I hereby give permission to publish the present thesis in accordance with the SLU agreement regarding the transfer of the right to publish a work.

NO, I do not give permission to publish the present work. The work will still be archived and its metadata and abstract will be visible and searchable.

